SUBMITTED TO
JOURNAL OF FLUIDS AND STRUCTURES

SYRINGOMYELIA: A REVIEW OF THE BIOMECHANICS

N.S.J. Elliott[1], C.D. Bertram[2]*, B.A. Martin[3], A.R. Brodbelt[4]

[1]Fluid Dynamics Research Group, Department of Mechanical Engineering, Curtin University Perth, Australia

[2]School of Mathematics & Statistics, University of Sydney Sydney, Australia

[3]Conquer Chiari Research Center, University of Akron Akron, OH, USA

[4]The Walton Centre NHS Foundation Trust Liverpool

* Corresponding author.
Email: c.bertram@sydney.edu.au
Phone: +61 2 9351 3646
Fax: +61 2 9351 4534

Contents

Abstract

Syringomyelia is a neurological disorder caused by the development of one or more macroscopic fluid-filled cavities in the spinal cord. While the aetiology remains uncertain, hydrodynamics appear to play a role. This has led to the involvement of engineers, who have modelled the system *in silico* and on the bench. In the process, hypotheses from the neurosurgical literature have been tested, and others generated, while aspects of the system mechanics have been clarified. The spinal cord is surrounded by cerebrospinal fluid (CSF) which is subject both to the periodic excitation of CSF expelled from the head with each heartbeat, and to intermittent larger transients from cough, sneeze, etc., via vertebral veins. The resulting pulsatile flow and pressure wave propagation, and their possible effects on cord cavities and cord stresses, have been elucidated. These engineering contributions are here reviewed for the first time.

Keywords: spinal cord, cerebrospinal fluid, Chiari malformation, spinal arachnoiditis, wave propagation, fluid-structure interaction.

List of acronyms

CNS	Central nervous system
CSF	Cerebrospinal fluid
ECS	Extracellular space
FSI	Fluid-structure interaction
HRP	Horseradish peroxidase
ISF	Interstitial fluid
MRI	Magnetic resonance imaging
PVS	Perivascular space
SC	Spinal cord
SSS	Spinal subarachnoid space

1 Introduction

The urge to analyse and understand the workings and malfunctions of the human body has led to intense development of particular areas of mechanics. These include wave travel in fluid-filled conduits (Grotberg and Jensen, 2004; Beulen et al., 2009), two-phase and multi-phase modeling of poroelastic media (Tully and Ventikos, 2011), pulsatile flow in laminar and transitional regimes (Stettler and Fazle Hussain, 1986), rheology of deformable-particle suspensions (Hoskins et al., 2009; Clausen et al., 2011), and time-dependent elasticity formulations for nonlinear solids undergoing finite deformations (Humphrey, 2003). Given the omnipresence in the body of soft tissue and relatively large structural deformations, fluid-structure interaction (FSI) is central to or intimately involved with all of these topics. Large-deformation FSI is quintessential to contracting cardiac muscle (Nash and Hunter, 2000; Peskin, 2002), but also inherent in the operation of cardiac (Watton et al., 2008), venous and lymphatic valves (Margaris and Black, 2012), collapsible conduits (Païdoussis, 2004; Chouly et al., 2008), and the larynx (Howe and McGowan, 2009). Heil and Hazel (2011) have recently reviewed prominent examples of physiological internal-flow FSI.

Analysis of such situations has given bioengineers tools with which to understand fluid flow and transport phenomena in other, less often studied parts of the body, including those filled with cerebrospinal fluid (CSF) which bound the brain and spinal cord. Using the concepts of wave travel and convective, viscous and diffusive fluid transport past and within deformable solid media, engineers have begun to contribute to understanding of medical problems of the CSF spaces in the body. One such problem is the subject of this review: syringomyelia.

Syringomyelia is a condition in which macroscopic fluid-filled cavities, called syrinxes[1], form and enlarge within the spinal cord (SC). Enlarging syrinxes often cause progressive neurological damage, through a combination of direct pressure on neural tissue, and ischaemia. The location of functional impairment depends on the site of neuronal damage. Syrinxes are most common in the cervical SC and this can lead to symptoms in both the arms and legs. Symptoms include chronic burning or aching pain, progressive muscle weakness and/or stiffness, numbness, and autonomic dysfunctions such as excessive sweating and bladder irritability. If the syrinx extends into the brainstem (syringobulbia) then coordinated oral functions, including chewing and swallowing, may also be lost.

Syringomyelia is associated with a number of different pathologies, although the great majority of cases can be related to either past spinal trauma or to Chiari malformation (Klekamp, 2009), in which congenital condition the base of the skull and part of the hindbrain combine to obstruct normal passage of cerebrospinal fluid (CSF) between the head and the spinal subarachnoid space (SSS). Idiopathic syringomyelia, although diagnosed in up to 16% of patients, may simply be a situation where the underlying cause is not visible with the imaging methods used (Sakushima et al., 2011). Treatment depends on the associated pathology and, to a degree, surgical preference, and is limited to surgical interventions that aim to reduce fluid pressure in the SC or improve freedom of flow in the surrounding subarachnoid space. This is achieved by variously removing bone (the lower back portion of the skull and/or the posterior part of the vertebra), draining the syrinx, inserting a shunt, and/or enlarging the enveloping soft tissue sheath (Klekamp and Samii, 2002). In the

[1] Some sources advocate syringes (Stedman's Medical Dictionary, 2006b) as the plural of syrinx, but the more commonly accepted form is syrinxes (Merriam-Webster's Medical Dictionary, 2006a).

majority of patients, such procedures stop further deterioration, and can relieve headache, but more rarely effect significant improvements. The SC has limited regenerative capacity and once neuronal damage occurs, symptoms are not relieved even with good syrinx control. Furthermore, most shunts fail eventually (Batzdorf et al., 1998), surgery can produce scarring that can lead to recurrence and worsening of symptoms, and even radiologically 'successfully treated' patients can deteriorate (Brodbelt and Stoodley, 2003; Levine, 2004).

Underlying this poor prognosis is a fundamental lack of understanding—the pathogenesis of syringomyelia (complicated by differing opinions on its clinical definition; Klekamp, 2002) has eluded physicians and surgeons for three centuries[2]. Not until the advent of magnetic resonance imaging (MRI) in the 1980s was even its diagnosis straightforward or reliable; see Fig. 1. In the majority of syringomyelia cases symptoms appear around 30 years of age and the condition progresses slowly (Boman and Iivanainen, 1967; Edgar and Quail, 1994; Moriwaki et al., 1995; Milhorat et al., 1999; Sakushima et al., 2011). There is a plethora of hypotheses for the causes of syringomyelia. Many of these hypotheses have since been contradicted by clinical evidence. The remaining candidates share recognition of a fluid-mechanical aspect to the disease progression, but the involvement of such physics has yet to solve the more puzzling aspects of syrinx formation:

- Syringomyelia typically consists of a single cavity yet there is no consistent containing mechanism; it is unclear why the tissue does not acquire many small cavities instead.
- According to some reports (Hall et al., 1980; Milhorat et al., 1997), but not others (Williams, 1976; Heiss et al., 1999), syrinx fluid has higher pressure than the fluid surrounding the cord from which it is apparently derived.
- Syrinx fluid accumulates extremely slowly relative to the timescales of hydrodynamic disturbances, such that it is difficult to rule out completely almost any mechanism of accumulation, even if it appears quantitatively infeasible.
- It is unclear whether a single mechanism underlies all syrinx development or if each spinal pathology is associated with a different one.

Phase contrast and magnitude MRI now provide useful quantitative information on pulsatile CSF flow and neurological anatomy, respectively. However, experimental description of the fluid mechanics remains incomplete because invasive pressure measurements are problematic. For this reason engineering modelling is an attractive option for investigating the biomechanics of syringomyelia. Engineering studies are relatively recent, and are reviewed here for the first time, focusing on their contribution to our understanding of the pathological mechanism of syringomyelia. Thus far they have (i) elucidated the nature of the pulsatile flow in a syrinx and in the space around the cord, including when stenosed, (ii) defined the effects of pressure waves, due to coughs or the cardiac cycle, on cord tissue stress and CSF/syrinx pressure, (iii) demonstrated some possible CSF pumping mechanisms, and (iv) helped to evaluate existing neurosurgical hypotheses. For brevity, we here review only studies that concentrate specifically on the SC. Spinal hydrodynamics are also simulated in models of the whole cerebrospinal system, such as the anatomically realistic 3D FSI model of Sweetman and Linninger (2011). However these models make few predictions that bear upon our understanding of syringomyelia with their focus being largely on the cerebral mechanics.

[2] Brunner (1700) reported on a newborn treated for syringomyelia.

2 Anatomy and physiology: structure and function

The salient features of the human cerebrospinal system are given, with emphasis on the SC. Except where specific articles are cited, this section is compiled from standard reference works (Gray, 1918; Marieb, 2000; Crossman and Neary, 2001; Martin, 2003; England and Wakeley, 2006; Guyton and Hall, 2006).

2.1 Gross anatomy

The SC lies in the upper two-thirds of the vertebral canal, the tubular space within the vertebrae. At the skull it joins and is continuous with the hindbrain. The SC (~ 40–45 cm long and 1 cm thick) transmits information to and from the trunk and limbs via 31 pairs of nerves which join the cord at intervals along its length. The vertebral column grows more than the SC, so the nerve roots in the lumbar and sacral regions descend almost vertically beyond the end of the cord to reach their exit points. This region is referred to as the *cauda equina* for its likeness to a horse's tail.

2.2 Meninges

The central nervous system (CNS—the cord and brain) is supported and protected by the vertebral column and the skull. Within this bony casing it is sheathed by three layers of membrane called the meninges (Fig. 2). The outermost membrane is the *dura mater*, a tough collagenous coat. The cranial dura is fused to the skull whereas the spinal dura is lubricated externally to allow articulation of the spine. On the inner surface of the dura is the *arachnoid mater*. Following trauma or other pathology, the arachnoid may be separated from the dura by a subdural space, but normally it is in direct contact. The arachnoid is a translucent, collagenous membrane named for the cobweb-like trabeculae (Sanan and van Loveren, 1999) that attach it to the *pia mater*, the innermost of the meninges. Mechanically, the arachnoid can normally be neglected in comparison with the dura, but it acquires importance through the inflammatory condition arachnoiditis (see below). The pia is a membrane of thickness of order 100 μm (Reina et al., 2004) that follows the surface contours of the brain and SC although cranially there is some evidence of a thin subpial fluid space (Zhang et al., 1990). Although thin, the spinal pia is mechanically important as the container of the scarcely solid tissue of the cord itself. The pia is perforated by the numerous blood vessels that enter or leave the CNS, and may have many other small fenestrations (Cloyd and Low, 1974; Reina et al., 2004). At its lower end the SC tapers conically and continues as the *filum terminale*, a rather elastic ligament of diameter ~1mm (Yamada et al., 2007) that anchors it to the first segment of the coccyx.

2.3 Material properties

CNS regions that are relatively rich in nerve cell bodies (e.g., the central portion of the SC and the surface of the brain hemispheres) are called grey matter. White matter contains mostly nerve fibres sheathed in myelin, an electrical insulator due to high fat content which confers a paler colour. Together the grey and white matter constitute the functional CNS tissue and are referred to as its parenchyma. Between these nerve cells is the extracellular space (ECS), consisting of tortuous, nanoscale pores (Gillies et al., 2002) filled with around 280 ml (Johanson, 2008) of interstitial fluid (ISF), about 20% of the CNS tissue volume (Nicholson, 1999).

The ISF and nerve cells form a poroelastic material[3]. Tracer studies in animals indicate that the grey and white matter permit bulk ISF flow (e.g., Wong et al., 2012), which may be anisotropic (Saadoun and Papadopoulos, 2010). However, the dominant mechanism by which excess fluid is eliminated from the cord remains obscure. The mechanics of the SC are complicated by the presence of travelling waves, which are not readily incorporated in a poroelastic formulation[4]. Therefore, analyses thus far of spinal FSI have modelled the SC parenchyma as a non-porous solid.

Salient data on the mechanical properties of spinal soft tissues are summarised in Table 1 (Tunturi, 1977, 1978; Chang et al., 1981; Hung and Chang, 1981; Hung et al., 1981; Hung et al., 1982; Tencer et al., 1985; Chang and Hung, 1988; Patin et al., 1993; Bilston and Thibault, 1996; Zarzur, 1996; Runza et al., 1999; Ichihara et al., 2001; Ozawa et al., 2001; Mazuchowski and Thibault, 2003; Wilcox et al., 2003; Ozawa et al., 2004; Oakland et al., 2006; Maikos et al., 2008; Ouyang et al., 2008; Saxena et al., 2009). Only simple indices such as Young's modulus are abstracted; some experiments (e.g., Sparrey and Keaveny, 2011) have yielded more sophisticated data on nonlinear or creep behaviour. The table shows a wide range of values for almost every parameter. Immediately relevant parameters for syringogenesis include cord resistance to transverse tearing (tensile stress), but compressive SC trauma may be implicated in fluid build-up (Saadoun and Papadopoulos, 2010). Only recent data make the important distinction between cord properties with and without the pia. While the circumferential and longitudinal stiffnesses of the spinal dura have been characterised in several species (in the process showing clearly its orthotropy), we lack data on the resulting compliance *in vivo*, where the dura is backed by fat and bone[5].

2.4 CSF spaces and circulation

Between the arachnoid and the pia is the subarachnoid space, filled with ~115 ml of CSF. The spinal subarachnoid space (SSS) is annular, has ~25 ml volume, and is traversed by nerves, by blood vessels, by fibrous trabeculae, and by the denticulate ligaments, two membranes running down the SSS as far as the second lumbar vertebra (Tubbs et al., 2001) which support the cord laterally. In terms of flow obstruction the trabeculae amount to irregularly spaced thin flexible posts. Trabeculae are more prevalent posteriorly and below the fifth cervical vertebral level, where they form a mesh-like septum (Nicholas and Weller, 1988; Parkinson, 1991; Vandenabeele et al., 1996; Fricke et al., 2001; Barshes et al., 2005; Mack et al., 2009). The denticulate ('saw-tooth') ligaments make continuous contact with the pia, and discontinuous contact with the arachnoid. The SSS enlarges at the lumbar cistern, between the conical end of the SC and the lower end of the filum. The subarachnoid space is also larger wherever the brain surface has a depression. At the craniocervical junction, where the spine

---

[3] If the blood vessels be included, the material can be thought of as multi-phasic. There have been attempts at modelling hydrocephalus using biphasic (e.g., Smillie et al., 2005) and recently multiple-network (Tully and Ventikos, 2011) poroelastic theories.

[4] See, e.g., an elementary biphasic model of cord parenchyma with/without a syrinx being loaded then unloaded (Harris and Hardwidge, 2010).

[5] The static compliance of the whole subarachnoid space decreases with filling, and in cats about one-third of the total CSF reservoir compliance resides in the SSS (Marmarou et al., 1975). Since it is likely that the majority of this third relates to the lumbar cistern, the segmental SSS compliance is probably much smaller. Dynamically it is almost certainly smaller again (Bertram, 2010).

articulates with the skull, there are two of these widenings, named the *cisterna magna* and the pontine cistern. The subarachnoid space is continuous with the four cavities of the brain called ventricles, of combined volume ~35 ml (Brodbelt and Stoodley, 2007), where most CSF is produced.

A tissue called the choroid plexus secretes the majority of CSF—essentially water, with minor additions of proteins, salts and sugars (Bloomfield et al., 1998). It flows from the two lateral ventricles down through the third and into the fourth ventricle, from where it exits the brain into the subarachnoid space, flowing around the SC and brain and finally being reabsorbed into venous blood via the arachnoid villi in the cranial subarachnoid space; see Fig. 3. An ill-defined amount of CSF is also derived from interstitial fluid (itself the result of capillary transudation and local metabolism) throughout the CNS. Some CSF is also absorbed indirectly into the lymphatic system (Brodbelt and Stoodley, 2007). Since both the main source and sink for CSF are located in the head, spinal CSF turnover seems to rely on a combination of lymphatic absorption, a few spinally located arachnoid villi, mixing due to postural changes, and local CSF derivation from ISF. Around 500 ml/day of CSF is produced in adult humans (Bradbury, 1993) and, as the CSF spaces have a total volume of about 150 ml, the fluid is replaced several times daily (Nolte, 2002). However this creeping mean flow is too slow to be measured by current MRI technology. The SC has a narrow conduit, the central canal (CC), with an opening to the fourth ventricle called the obex, but in health the CC almost disappears by adulthood (Milhorat et al., 1994). CSF provides buoyancy and a hydraulic cushion for the brain and SC[6], and exchanges substances between the brain and the rest of the body.

2.5 Cerebrospinal blood supply and CSF interactions

The brain receives its blood supply from the left and right internal carotid and vertebral arteries, which join together to form the circle of Willis. The SC is supplied by branches from the vertebral arteries that feed into the cranial end of the anterior and paired posterior spinal arteries. Along their length the spinal arteries also receive flow from branches of mainly the intercostal arteries (Martin et al., 2012). The arteries and veins serving the brain and SC run for part of their course in the subarachnoid space, where they are exposed to CSF pressure.

In the human brain parenchyma and cranial subarachnoid space electron miscroscopy has revealed that the arteries reside within tubular sheaths that extend inward and outward, respectively, from the pial surface, while the veins lose their pia-like sheaths once they enter the parenchyma (Zhang et al., 1990). It seems probable but not certain that the situation is the same in the spinal canal. The annular fluid-filled spaces surrounding these vessels at the parenchyma level are called perivascular spaces (PVS)[7]; see Fig. 4. Cerebrospinal and interstitial fluids may pass through pores and leaky gap junctions in the otherwise apparently continuous pia although the viscous resistance may be lower within the perivascular sheaths themselves. Tracer studies have tracked CSF flow inward through the spinal pial membrane and bidirectionally through the cranial pial membrane (Rennels et al., 1985). The ECS, the PVS and the subarachnoid space are thus a single continuous fluid compartment (Rennels et al., 1985; Stoodley et al., 1996; Johanson, 2008; Saadoun and Papadopoulos, 2010). It has been estimated that 10–30% of total CSF flow is associated with fluid secreted from the walls of the brain microvessels (endothelial cells) into the PVS (Redzic et al., 2005). In addition, blood plasma may be filtered into the PVS through these walls (the so-called blood-brain/SC

[6] Demonstrated in the computational FSI models of SC trauma of Persson et al. (2011).

[7] Also called Virchow-Robin spaces.

barrier) under the influence of a pressure or concentration gradient. Accumulation of the same filtrate within the nerve cells and/or ECS leads to tissue swelling, referred to as oedema (Saadoun and Papadopoulos, 2010). In the brain this fluid is evacuated into the subarachnoid and ventricular CSF, the latter involving passage through gaps between the ependymal cells that line the ventricles (Johanson, 2008; Saadoun and Papadopoulos, 2010). There is a dearth of evidence on the porosity of the CC ependyma (Wong et al., 2012).

The heartbeat and breathing cycle are transmitted to the CSF through the time-varying distension of arteries and veins, respectively, superimposing a pulsatile component over the slow mean flow of CSF in the subarachnoid space and ventricles. The transmission is particularly efficient in the head, where the constant skull volume, along with the incompressibility of the water-saturated contents, ensures CSF displacement with arterial volume change. At the craniocervical junction, the pulse pressure is of order 67–330 Pa (0.5–2.5 mmHg; Takizawa et al., 1986; Heiss et al., 1999; Park et al., 2010), and the stroke volume is 0.35–1 ml (Wagshul et al., 2006). However, in dogs less than a quarter of lumbar CSF pulsatility is reported to be of cranial origin (Urayama, 1994), and evidence suggests a similar situation in humans (Henry-Feugeas et al., 2000).

3 Biological hypotheses

To understand why current hypotheses for the aetiology of syringomyelia focus on hydrodynamics, it is necessary to review briefly the more biological theories that have been considered and in large part abandoned. Only the theories themselves are listed here; more detailed review, including the evidence against them, is given elsewhere (Tauber and Langworthy, 1935; Williams, 1980; Klekamp, 2002).

Syrinxes were observed early on at sites of congenital malformation such as *spina bifida* (a hernia of the meninges and sometimes the cord through a cleft spinal column), leading to the idea that the syrinx was part of the congenital defect (Morgagni, 1769; Ollivier D'Angers, 1827). The concept was moved to the micro scale by Hinsdale (1897), who proposed that syringomyelia constituted a developmental defect of the (glial) cells lining the CC and between the nerve fibres.

An idea popular from the mid-1800s to the late 1920s was that a glial tumour, acquired *in utero* or postnatally, cavitated due to insufficient blood supply (Riley, 1930). This neoplastic concept suggested therapy by irradiation. However it was found (Tauber and Langworthy, 1935) that the cavity was typically surrounded by neural (glial) scar tissue rather than tumour cells. Eventually it was shown that radiotherapy made no difference to the long-term course of syringomyelia (Boman and Iivanainen, 1967).

In parallel, there was speculation that swelling due to meningitis (Charcot and Joffroy, 1869; Joffroy and Achard, 1887) or just Chiari malformation (Lichtenstein, 1943; Tarlov et al., 1953; McGrath, 1965; Martinez-Arizala et al., 1995) could lead via venous obstruction and/or arterial clotting to ischaemic damage in the SC which became syringomyelia. However animal models of ischaemia tended to produce SC softening (myelomalacia) rather than cavitation.

Another blood-based theory was that syringomyelia developed from a SC haematoma caused by trauma (Bastian, 1867). The clot was thought to liquefy becoming a syrinx; i.e., the two cavities were thought to be one and the same. Many animal models followed, using various methods to inflict SC trauma. All yielded a lesion of the SC and a SC cavity at the level of the

trauma (Brodbelt and Stoodley, 2003). Although post-traumatic cysts are often present at the site of injury, most clinicians would distinguish them from a syrinx, which enlarges, causes progressive symptoms, and will often extend beyond the site of injury (Brodbelt and Stoodley, 2003). It may be that a haematoma provides the initial fluid-filled cavity that will go on to form a syrinx sustained via a separate mechanism, but only a minority of such patients will develop a syrinx.

An imbalance between fluid delivery (by bulk flow or local secretion) and drainage in the cord has long been suggested as a possible cause for syringomyelia (Morgagni, 1769; Barnett, 1973). The measured similarity of syrinx fluid to CSF led some to the conclusion that ependymal cells, which line the CC and ventricles, secrete CSF which accumulates and causes a syrinx if the CC is obstructed (Rice-Edwards, 1977; Wiedemayer et al., 1990). However, in humans the CC appears to occlude with age in the vast majority of healthy individuals (Kasantikul et al., 1979; Milhorat et al., 1994), whereas syringomyelia is uncommon. Nevertheless, other imbalances are not ruled out, and even today, knowledge of SC micro-venous anatomy and function lags behind that of the equivalent arteries.

It has also been postulated that a syrinx arises by permeation of fluid under pressure from a primary lesion which might be trauma-induced (Holmes, 1915) or a cystic tumour (Williams, 1970, 1980, 1986; Lohle et al., 1994). In cases of cystic tumours of the cervical SC (Gardner, 1965), syrinx fluid was "thick and yellow", with a protein content two orders of magnitude higher than CSF. This idea would account for occasional cases of patients diagnosed with syringomyelia benefitting from radiotherapy. Although a third to a half of SC tumours have an associated syrinx (Samii and Klekamp, 1994; Yang et al., 2009), the idea does not explain why syringomyelia is more frequently associated with tumours at the cervical level than those lower down the cord (Samii and Klekamp, 1994).

However, as might be expected, biological hypotheses continue. A recent example is a candidate explanation for post-traumatic syringomyelia as the result of fluid leaked from the microcirculation in the presence of a compromised blood-SC barrier (Hemley et al., 2009) after syrinx creation by injection of excitotoxic amino acids in rats.

4 Mechanical hypotheses from neurosurgery

The neurosurgical literature has a history of theories of syringomyelia involving largely hydrodynamic mechanisms, going back to 1950 (Gardner and Goodall). These hypotheses are frequently quite complex, combining in an overall causal chain many different steps, some more reasonable than others. They often intersect, such that the same postulated physical process may be invoked to support more than one theory. The earliest theories (Gardner and Angel, 1959) have now been discarded, as hypothesizing situations that did not conform to what was typically found clinically (Ball and Dayan, 1972; Williams, 1980). Each surviving theory is here outlined and an attempt is made to distil the individual physical processes involved. In subsequent sections we assess to what extent each of these processes has been verified by engineering studies.

4.1 Pressure dissociation (Williams)

While credit for first drawing attention to hydrodynamic mechanisms must go to the American neurosurgeon Gardner and his colleagues (Gardner and Angel, 1959), it was an English neurosurgeon, Williams, who first sought to interest engineers in the fluid-mechanical analysis of syringomyelia. Williams held that, to explain the pathological findings, a

mechanism must set up a significant pressure difference between the inside and outside of the cord without altering the difference in pressure between the inside and outside of the brain. He believed that venous pressure transients caused by coughing or sneezing were the main driving force behind displacement of CSF from the cranium to the spinal canal. He proposed two mechanisms pertaining to syrinx pathology, one for formation and another for expansion, termed 'suck' and 'slosh' respectively. These hypotheses contain much that is physically reasonable, if not uniformly so. Williams supported his ideas with invasive pressure measurements on conscious humans (Williams, 1972, 1976). Such procedures are rarely performed (Häckel et al., 2001), and the data remain invaluable empirical evidence.

Lumbar and cisternal pressures were recorded simultaneously. Cough impulses of 1.3–12.9 kPa (10–97 mmHg) peak-to-peak amplitude were measured, and the pressure wave speed was estimated[8]. The cisternal wave always arrived after the lumbar wave, with a lesser amplitude, and was of longer duration. All of these features were more pronounced when there was a partial SSS blockage. The pressure recordings were interpreted as demonstrating the *craniospinal pressure dissociation* mechanism, later termed suck[9] (Williams, 1980). Referring to Fig. 5(a), the differential pressure trace shows that, after the cough pulse passes the cisternal transducer, the cranial and spinal compartments become dissociated—a negative pressure acts across the hindbrain, reaching a minimum of around –1.3 kPa (–10 mmHg) and decaying over half a minute. This suction pressure, ascribed to the hindbrain plugging the SSS, would tend to induce CSF to flow from the head into the CC (as per Williams, 1990, fig. 7), i.e. the hindbrain hernia acted as a one-way valve. The dissociation effect was more pronounced when the patients performed a Valsalva manoeuvre (Fig. 5(b))—an attempted expiration against a closed glottis after a full inspiration—and such manoeuvres sometimes exacerbated their symptoms. Dissociation was also observable when the SSS blockage was due to a tumour within the SC (Williams, 1980, fig. 3).

The slosh mechanism was suggested for the longitudinal expansion of an existing syrinx. Compression of the SSS due to distension of the epidural veins tends to squeeze the SC, forcing the syrinx fluid to be displaced upwards. This fluid movement was observable with X-ray contrast medium in the syrinx. The surge of fluid[10] was thought to damage the SC tissue and thus elongate the syrinx cavity; a similar but diminished effect was posited for the downward direction.

Suck required a patent connection between the CC and the fourth ventricle. Instances of 'non-communicating' syrinxes were assumed to involve tumour exudate (Williams, 1969, 1970). Williams later dismissed perivascular flow as a source of syrinx fluid, stating that "Fluid may not … be forced along the perivascular spaces to initiate or inflate a syrinx because uniformly

---

[8] The SSS wave speed was subsequently shown (Greitz et al., 1999; Kalata et al., 2009) to be around 5 m/s, considerably lower than he estimated; see Bertram (2010) for discussion of the subject. Recent (as-yet unpublished) measurements by Loth suggest wavespeeds at the craniospinal junction as low as 3 m/s.

[9] The full suck hypothesis, including anatomical assumptions, must be distinguished from pressure dissociation alone. Pressure difference always accompanies flow past a SSS stenosis. Williams had in mind here the longer-lasting pressure dissociation seen in his measurements *in vivo*.

[10] Williams used 'slosh' to convey the sense of the syrinx fluid motion, not the splashing sound and implied free fluid surface of the onomatopoeic everyday use of the word.

raised pressure around the cord must tend to compress rather than expand it" (Williams, 1980)—see §5.6. However, this thinking was revised when he sought to account for post-traumatic syringomyelia. If the SSS blockage was caused by subarachnoid scar tissue, he reasoned (Williams, 1986), SSS pressure waves during coughing will force upward fluid movement past the obstruction both inside and outside the cord, and in the recovery period fluid will be sucked into the cord directly through the cord tissue, causing distension of the lower part of the cavity and fluid build-up.

Earlier, Williams (1974) built a physical model of the craniospinal fluid system and interacting organ systems to support his theories. He was able to demonstrate craniospinal pressure dissociation through 'coughing' as a result of the hindbrain hernia valve, and filling of a communicating syrinx whenever the intrasyrinx pressure was lower than intracranial pressure (ICP). Increasing SSS compliance damped intraspinal pulsations and weakened the pressure dissociation.

The syrinx container retained all fluid received because of an additional valve in the model, corresponding to one presumed to operate in the upper CC due to external compression of the SC by the hindbrain. This valve appeared to have a functional equivalent in dogs (Hall et al., 1980) but the purpose of the CC hence any associated valve, although not completely understood (Storer et al., 1998), is now thought to be species-specific.

4.2 Piston (Oldfield/Heiss)

Oldfield et al. (1994) formulated a theory for syrinx formation and progression based on perivascular flow. They proposed that systolic pulsations in the head create a piston-like action on the hindbrain which excites caudal-moving pressure waves that squeeze the SC, forcing fluid into the SC via the PVS to originate a syrinx, and propelling intra-syrinx fluid downwards maintaining its progression. In support of their theory Heiss et al. (1999) presented a study of healthy subjects and patients with Chiari malformation and signs of syringomyelia. MRI (static and dynamic), ultrasound and invasive pressure measurements were taken. Compared to the volunteers, the patients had obstructed CSF flow and impaired pressure transmission between the head and spinal canal, and the SSS had lower compliance. Flow in the SSS was downward during systole and upward during diastole, synchronous with hindbrain movements. Syrinx compression coincided with raised SSS pressure and descent of the hindbrain. Gross deformations of the SC and syrinx cavity were observable with intraoperative ultrasonography. Patients were treated by decompression of the hindbrain but the syrinx was left intact. After surgery the piston-like action of the hindbrain ceased, SSS compliance increased, pressure and flow characteristics normalised, and the syrinx diameter decreased. Symptoms tended to persist, but this was attributed to irreversible SC damage.

They found that the syrinx tended to be compressed during systole, which argued against early hydrodynamic theory (Gardner and Angel, 1959), and that the syrinx diameter did not increase during the Valsalva manoeuvre as predicted by Williams. The piston hypothesis was later taken up by Fischbein et al. (1999, 2000)—see §7.2. It postulates a failure process for spinal tissues involving eventual yielding to stresses which are far below any short-term threshold for damage. This idea is not backed up by evidence.

4.3 Intra-cord pulse pressure (Greitz)

Greitz and co-workers (Greitz, 1995; Greitz et al., 1999; Josephson et al., 2001; Greitz and Flodmark, 2004; Greitz, 2006) presented an ambitious attempt to explain the pathogenesis of syringomyelia in all its guises, i.e. in association with Chiari malformation, spinal trauma or arachnoiditis, as well as occurring secondary to tumours in the spinal canal or the base of the

skull. The emphasis was on the pulse pressure of capillaries within the SC.

The proposed mechanism rested on ideas about the separate propagation of pressure waves—one in the SC and another in the CSF in the SSS—which were developed diagrammatically (e.g., Greitz, 2006, fig. 1). The proposal also emphasized a Venturi effect in the SSS, which was thought to cause suction on the SC and so act to distend it. In support of this idea, Greitz's group presented dynamic MRI measurements in humans showing CSF velocity increases of up to four times, with peak ~80 mm/s through a partial SSS obstruction (Greitz et al., 1999). In animal experiments, constriction of the SSS by ligature led to syrinxes forming at adjacent sites above and below (Josephson et al., 2001; Greitz and Flodmark, 2004); these outcomes were interpreted as supporting the separate-waves part of the theory. However, Milhorat, in an appendix to Josephson et al. (2001), comments that the ligature almost certainly also caused SC ischaemia, leading to the acute paraplegia which was seen in surviving animals. Both the wave and the Venturi aspects of the proposal have now been questioned following engineering examination.

5 Analysis of the neurosurgical hypotheses

In this section we describe the extent to which the physical processes associated with wave propagation, syrinxes, stenoses, etc., have been verified by engineering studies. These are employed to assess the merits of the above neurosurgical hypotheses.

5.1 Waves

The SSS and its bounding structures, including a part of the SC with a syrinx, can be thought of as a pair of coaxial thick-walled fluid-filled elastic tubes. Such a system supports four modes of wave propagation (Bertram, 2009; Cirovic, 2009). In order of increasing wave speed these are as follows (using descriptors related to the present topic).

1. What is normally thought of as the SSS pressure pulse wave, also comprising radial cord compression and dura distension.
2. A wave causing outward deflection of both cord and dura, and axial cord tension.
3. A wave superficially similar to wave 2 but causing cord axial compression.
4. A wave almost entirely confined to axial tensile stress and deformation of the dura.

In the absence of a syrinx, this system can also be interpreted as relating to a cord with patent CC. As the inner fluid conduit shrinks to negligible diameter, waves 1 and 2 progressively acquire similar speed (Cirovic, 2009; Cirovic and Kim, 2012), and in the limit of no CC or syrinx, combine; the system then supports only three wave types: the pressure pulse in the SSS (approximating the Young wave in a non-annular conduit), an intermediate-speed wave of mixed type, and a Lamb wave of axial tension in the dura.

The important waves involve the interaction of the elastic solids with the dense fluid; Greitz's concept of separate waves in the cord and the CSF does not hold. Reflection, refraction and subsequent interaction of the various waves in the spinal canal at the borders of a syrinx are complicated (e.g., Bertram, 2009, fig. 10) even before involving a partial SSS obstruction, and do not lend themselves to intuitive theorizing. However the papers from Greitz's group have sparked much interest and discussion.

5.2 Syrinx

When a syrinx is present, the contained fluid is stirred into motion by the progressive deformation of the cord as a pressure wave is transmitted along the spinal canal. The numerical model of Bertram (2009) demonstrates this; the rostrocaudal propagation of pressure waves in the SSS induces axial motion of the syrinx fluid relative to the syrinx walls, of comparable magnitude to that measured *in vivo* (Heiss et al., 1999; Brugières et al., 2000). The motion also leads to fluid pressure at the caudal end of the syrinx exceeding SSS pressure at the same level, and tensile radial stress at the caudal tip of the syrinx wall, i.e. arresting the momentum of the syrinx fluid incurs stress in the cord with potential to tear the tissue. Although pressure waves slow down significantly past the syrinx, as predicted analytically (Cirovic, 2009), they remain much faster than the relative axial fluid motion achieved in the syrinx, producing rather ineffective peristaltic action on the syrinx contents (Bertram, 2009). The effects of the syrinx (slowed wave speed, peristaltic syrinx flow, raised end pressures, raised cord radial stress) were reduced when the homogeneous SC was differentiated into a thin tough pia and softer cord tissue, showing a protective role for the pia (Bertram, 2010).

The modest magnitude of the effects suggested that slosh-induced tissue dissection, proposed by Williams (1980) and taken up by Oldfield et al. (Oldfield et al., 1994), could not induce immediate syrinx expansion. However, although the geometrical and material property values used were reasonable and the wave-speed/fluid-speed disparity agrees with clinical measurements (Bertram, 2009), the magnitude of the simulated excitations (0.1 or 1 kPa; 0.75 or 7.5mmHg) was small compared to maximum recorded CSF pressures when coughing (10 kPa; 75 mmHg). Linear extrapolation of the results (scaling up) is possible but incurs further approximation owing to nonlinearity of the FSI and *in vivo* material properties. The stress concentration at the ends of the syrinx was also under-resolved.

5.3 Subarachnoid stenosis

The first engineering investigation of a pressure wave propagating in a stenosed SSS was by Lockey et al. (1975). In their 1D analysis the dura was flexible, the SC was rigid, the SSS fluid inviscid and the stenosis a rigid attachment to the SSS surface. The speed of the radial expansion wave of the dura was chiefly determined by the thickness of the dura, this being the only source of compliance. The wave slowed with increasing SSS blockage, but the effect on SSS pressure was not obtainable. This information is provided by more recent physical (Martin and Loth, 2009; Martin et al., 2010) and computational (Bertram, 2010) modelling. In their physical models without a syrinx, Martin and colleagues (Martin and Loth, 2009; Martin et al., 2010) also had only one source of compliance, but chose this to be the SC (a silicone polymer); an annular flow obstruction was attached to the rigid dural surface at an intermediate location. When excited by a flux impulse to the SSS representative of percussive (Martin and Loth, 2009) or cardiac-like (Martin et al., 2010) CSF pulsation, the stenosis attenuated the amplitude of passing CSF pulsations, and transients were set up of alternating positive and negative pressure difference between the ends of the model. In a computational model that had an elastic dura as well, Bertram (2010) found that the system behaved very differently depending on the timescale of the initial perturbation. Brief excitation, either cranially or abdominally, produced mainly wave propagation rather than bulk fluid motion along the SSS, hence little pressure differential across a subarachnoid stenosis, irrespective of severity. Conversely, cardiac-timescale transients generated pressure gradients that mostly had to do with acceleration of fluid along the SSS. This is an important finding, as most intuitive clinical/qualitative theories, including all three from neurosurgery described above (§4), assume that pressure wave propagation and bulk fluid motion go hand in hand.

The complex three-dimensional narrowing of the subarachnoid space at the craniospinal junction which is the result of Chiari malformation has received much attention, particularly from Haughton and colleagues, in terms of MR measurements of CSF velocity and computational fluid flow simulation (Roldan et al., 2009; Hentschel et al., 2010; Linge et al., 2010). The condition is often attended by flow heterogeneities including vortices and jets (Bunck et al., 2011). In general the small velocities make accurate measurement of the CSF flow field challenging (Santini et al., 2009; Battal et al., 2011; Odéen et al., 2011). Readers are referred to a detailed recent review (Shaffer et al., 2011).

5.4 Syrinx and subarachnoid stenosis

In Martin and colleagues' experiments on physical models with a flexible SC, when a syrinx was included in combination with a co-located subarachnoid stenosis and the excitation was a cardiac-like pulsation, there were pronounced swings in SSS pressure difference across the stenosis. The trans-stenosis pressure difference caused the syrinx to be compressed at one end and dilated at the other, which tended to narrow the SSS passage past the stenosis. During diastole the stenosed passageway transiently offered higher resistance to flow, thus forming a dynamic valve between the syrinx wall and the stenosis; a caudorostral (rostral: directed toward the head) tension was also induced in the SC. This valve did not feature in the experiments with a simulated cough. The presence of the syrinx tended to reduce the pressure differential acting across the obstruction (Martin and Loth, 2009). In a further model with flexible dura and therefore increased SSS compliance, the pressure pulse (amplitude and mean value) was damped and consequently the pressure differential was reduced.

Bertram's (2010) simulations also predicted this one-way valve mechanism[11], elevating mean SSS pressure caudal to the stenosis and causing axial translation of the cord in the cranial direction, even though only partial valve closure occurred. Flow past the stenosis was allied to substantial pressure dissociation in the SSS. When the excitation was an arterial transient, stenosis caused rapid decay of the to-and-fro fluid motions and associated pressure swings after the transient. There were small movements of fluid in the syrinx (in line with published *in vivo* measurements) but stenosis increased this motion only somewhat. The decoupling between SSS pressure dissociation and syrinx fluid motion (slosh) was due to a difference in time scale between relatively immediate responses of syrinx fluid to external forces and the rather slow characteristic frequency of to-and-fro motions of fluid in the SSS. For related reasons, quick SSS transients (exciting shorter-wavelength cord displacements) were more efficient in creating syrinx fluid motions, although also more rapidly damped. Bertram's (2010) computations for a syrinx with an adjacent stenosis predicted that radial tensile stress in the cord could reach 80% of the magnitude of the initial pressure transient.

Martin et al. (2010) also constructed a physical model in which the obstruction was positioned rostral to the syrinx, representative of a Chiari malformation. No one-way valve action was recorded but the obstruction was not able to move independently of the dura and plug the SSS. Pressure dissociation at the craniocervical junction, as proposed by Williams (1980), may be fundamentally different than at a subarachnoid stenosis due to the ability of the hindbrain to move independently of the cord and dura and its more intimate involvement with the cranial CSF dynamics.

---

[11] Chang & Nakagawa (2004) had also predicted a raised SC pressure with respect to the SSS just below the obstruction.

Alternating distension and compression of the ends of a syrinx with an overlying stenosis, as suggested by Greitz (2006), is borne out in bench-top (Martin and Loth, 2009; Martin et al., 2010) and computational (Bertram, 2010) studies. However, reasoning qualitatively, Greitz (2006) predicted the opposite SSS valve action at the site of a syrinx to that which occurred in the physical and numerical models.

5.5 Venturi effect

Greitz (2006) proposed much significance for a Venturi effect, but the idea was not backed up by measurements of pressure or cord displacement. The thinking behind the hypothesis neglected viscous losses and the dominance of unsteady flow-driving pressure changes in the SSS. These lead to substantial deviations from Bernoulli's eighteenth-century insight based on steady potential flow.

In their bench-top experiments Martin and colleagues found that the Venturi effect was negligible for both percussive (Martin and Loth, 2009) and simulated cardiac (Martin et al., 2010) CSF excitation, even with >90% flow stenosis. For cardiac input in the rigid-dura model with a syrinx, CSF pressure in the SSS did not recover downstream of the obstruction. When a syrinx was present the mean pressure at the stenosis site increased, contrary to prediction on the basis of Venturi (Martin et al., 2010). The unsteady nature of the flow dominated the fluid mechanics. For the simulated cough experiments SSS pressure only recovered slightly downstream to the stenosis when the dura was flexible. The outward ballooning of the syrinx did not require a Venturi effect, only a decrease in overall SSS pressure while syrinx pressure remained uniform (Martin and Loth, 2009). In contrast, the computational results of Bertram (2010) did demonstrate a small outward cycle-average radial displacement of the cord surface under the stenosis due to a Venturi effect when excited by periodic cardiac-frequency pressure pulsations. This was pronounced only at the cranial margin of the stenosis where the gap was particularly small at one phase of the cycle; a stenosis that did not deform with the dura would have occasioned even less effect.

5.6 Forcing fluid into the cord

The neurosurgical hypotheses include various suggestions about the forcing or drawing of SSS fluid into the cord tissue based on intuition rather than strict physics. The situation is complex, since the tissue is poroelastic (includes a non-bound fluid component) and its borders at the pia (and for present purposes at the glial surface of a syrinx) are variously semi-permeable. However, one statement can be made with certainty. As pointed out by Carpenter et al. (2003), elevated SSS pressure will tend to constrict the SC and drive fluid out; this fluid would be recovered, at best, upon relaxation of the cord deformation—demonstrated by the subsequent analytical model of Elliott (2012). Fluid cannot be 'squeezed' into the cord (Carpenter et al., 2003); in the absence of a pumping mechanism it can only be drawn in as the cord dilates.

6 Hypotheses from engineering

This section describes hypotheses derived from mathematical analysis or numerical modelling that were later assessed as unlikely.

6.1 An analogue of the hydrodynamic hypothesis

Medical evidence casting doubt on Gardner's hypothesis (Gardner and Angel, 1959) predates most engineering attempts at modelling syringomyelia. Consequently, the lumped-parameter

models of Chang and Nakagawa (2003, 2004) remain the only computational models to have included a connecting fluid passage (obex) between the fourth ventricle and a patent CC. They adopted an electric circuit analogue, with cranial chamber pressures represented by voltages. The CC and SSS fluid conduits were each represented by a series of resistors, connected at the caudal end; an additional resistor simulated the obex. Compliance ascribed to axial segments of the SC and dura was represented by capacitors, and two further capacitors represented the compliances of the lumbar cistern and the cisterna magna. By exciting the model with an impulse between the fourth ventricle and prepontine cistern and observing that the CC pressure became transiently elevated as the cisterna magna compliance was reduced, Chang and Nakagawa were led to suggest that the cisterna magna acts as a "shock absorber" against the pulsatile CSF waves from the cranium, and that the loss of this compliance due to crowding of the base of the skull (Chiari) causes an increase in the pressure in the CC, leading to syringomyelia. In other words, their predictions supported the hydrodynamic hypothesis.

Chang and Nakagawa (2003) gave little justification for the physiological parameter values used, which spanned 10 orders of magnitude, on the grounds that they were only interested in qualitative behaviour. However, the relative size of the various parameters is still of importance. The second model (Chang and Nakagawa, 2004) was a modification to simulate flow obstruction in the SSS.

6.2 Elastic jump (Carpenter)

Carpenter and colleagues presented a hypothesis for syringomyelia pathogenesis (Berkouk et al., 2003; Carpenter et al., 2003) based on a model consisting of a pair of fluid-filled coaxial tubes, the inner one being flexible, the outer rigid, and the enclosed and intervening fluid inviscid. The outer tube represented the dura and surrounding structures and the annular fluid space corresponded to the SSS. The flexible tube was originally interpreted as the SC and the fluid space within was thus the CC (Carpenter et al., 1999; Berkouk et al., 2003). The flexible tube was later reinterpreted as the pia, with the contained fluid approximating the SC tissue (Carpenter et al., 2003).

They developed a weakly-nonlinear theory for propagation of long small-amplitude pressure waves (Berkouk et al., 2003). The wave speed was a strong function of the ratio of the tubes' cross-sectional areas. They showed that the leading edge of a pressure pulse steepens to form a shock-like elastic jump, a phenomenon akin to a beach wave breaking as it reaches shallow water. When such an elastic jump reflected from a complete blockage of the SSS it formed a localised transient of amplified transmural pressure, greater than the doubling predicted by linear theory. *In vivo* the effect would be strongest for a hindbrain stenosis and cough-induced pressure disturbance, and it was proposed (Carpenter et al., 2003) that this might elevate the pressure within the SC sufficiently to cause tissue damage and generate a syrinx. The importance of the theory was its potential to explain how input pressures might be greatly scaled up.

The elastic-jump hypothesis has subsequently been shown to be quantitatively implausible. Elliott et al. (2009) determined the dependence of both the distance required for an elastic jump to form, and the pressure amplification factor of a subsequent reflection, on the geometry of the cord and dura. Since the SC cross-sectional area is far from the asymptotic limits (negligibly sized SC or SSS) of the theory[12], a distance of 10–100 cord lengths would be

[12] Just as well, as the viscous forces which were ignored become non-negligible as the asymptotic limit is approached (Elliott et al., 2009).

required for the pressure pulse to form an elastic jump, and the amplification would then only be a few percent greater than linear doubling, less than the measured attenuation of cough impulses (Lockey et al., 1975). Elastic jumps are thus unlikely to be of significance in the SSS.

However, the elastic jump theory approximated the SC crudely. Could shock-like phenomena feature in a more realistic model? Bertram et al. (2005) investigated this in a numerical model where the SC and dura were both homogeneous linear elastic solids, and the fluid was viscous. The system was excited with pressure impulses equivalent to arterial pulsation and coughing, then the wave propagation and reflection were observed. At cardiac frequencies the dynamic response was close to that of a lumped system with the pressure along the length of the SSS rising and falling almost in synchrony. A more distributed response was observed at the higher frequencies found in cough pulses. However, at no frequency studied did the wave speed fall sufficiently low for the SC to be long relative to the wavelength. The pressure pulse tended to flatten as it propagated (dispersion). On this basis syringogenesis by shock formation is again unlikely (Bertram et al., 2005).

6.3 Peristalsis (Bilston)

Bilston et al. (2003) proposed that the pressure wave travelling down a spinal artery sets up a peristaltic flow into the SC through the surrounding PVS. The PVS was modelled as an axisymmetric annular fluid conduit, with the pressure pulse in the contained spinal artery as a prescribed travelling wave of inner wall deformation. The chosen parameters predicted pumping against a syrinx pressure of 3.6 kPa (27 mmHg) that it was estimated could expand the CC from a diameter of 1 mm to 1.6 mm. Thus there was a mechanical explanation for how CSF could flow 'up-hill' from the SSS to form a syrinx.

A parametric sensitivity analysis was performed of the 'wave' shape, speed, amplitude and wavelength, but there was no physical justification for the range of values investigated (Bilston et al., 2003). The assumed arterial wall pulse had a wavelength[13] of 19–60 μm, and these pulses occurred 100–300 μm apart along a perivascular artery of diameter 100 μm. However, in reality, the wavelength of the arterial pulses generated by cardiac action is extremely long relative to the dimensions of the PVS. For such waves the peristalsis would be inefficient to vanishing point.

Abandoning this hypothesis, Bilston's group later demonstrated another perivascular pump, which would work with long waves (Bilston et al., 2007; Bilston et al., 2010); see §7.7.1.

7 Current status

Much has been learned about the mechanics of syringomyelia through engineering investigations, but there are still many open questions. Theoretical models can have contradictory elements yet not be mutually exclusive, when they propose mechanisms based on different aspects of the overall physics. As each model is tailored to the physics it seeks to elucidate, a model designed to demonstrate one mechanism is not necessarily well suited to evaluate another. For this reason it is not always possible to resolve differences between them. What follows is a partial synthesis of the current state of knowledge.

7.1 The nature of CSF flow

[13] Determined as the length enclosing 99% of the given pulse height.

Pulsatile CSF flow in the SSS is laminar; Loth et al. (2001) computed Reynolds numbers in the range 150–450. It is largely inertia-dominated; Womersley numbers of 5–17 and rather flat velocity profiles were found in a CFD model based on anatomical geometry (The Visible Human Project®, U.S. National Library of Medicine), which is consistent with analytical predictions from measured CSF flow rates (Gupta et al., 2008). Stockman (2006) has shown in a lattice-Boltzmann model that the structures which inhabit the SSS (nerves, trabeculae and ligaments) modify the flow only slightly, although modelling of the cranial subarachnoid space as a Brinkman porous medium (Gupta et al., 2009) suggested that they increase flow resistance significantly. In the intact cord viscous forces dominate the interstitial fluid transport (Elliott, 2012) but these give way to inertial forces in syrinxes occupying the greater part of the cord diameter (Bertram, 2010). Transport by mixing is more important in the SSS than mean flow (Greitz and Hannerz, 1996; Stockman, 2007). Taylor dispersion greatly augments drug transport along the SSS (Hettiarachchi et al., 2011). However consensus on quantitative indices for abnormal CSF flow and pressure in the SSS has not yet been reached.

7.2 How does an extracanalicular cavity first arise?

Fischbein et al. (1999, 2000) suggested that there may exist a normal dynamic equilibrium of flow between the SSS and SC via the PVS. The normal situation was also assumed to include a CC divided into isolated segments. It was argued that if the SSS pressure is periodically raised by systolic pulsations of a hindbrain hernia then there may be a net inflow of CSF into the SC (but see §4.2). Patent segments of CC were thought to inflate to form syrinxes, but if no such segments existed then CSF would diffuse into the cord tissue resulting in oedema and cord swelling. Noting the similarity on MRI of oedema and syrinxes, they proposed that SC oedema was a reversible "pre-syrinx" state. However, while mechanisms of oedema formation and resolution in the SC are not well understood, if similar to those operating in the brain then the excess fluid seems more likely to originate from the SC vascular system (Saadoun and Papadopoulos, 2010).

Stoodley and colleagues proposed that adhesive arachnoiditis might potentiate syrinx formation by CSF flow obstruction, cord tethering and/or a change in SSS compliance. They examined (Brodbelt et al., 2003c) the effects of altering global SSS compliance by shunting the CSF from the lumbar cistern into the abdomen whilst maintaining the localised effects of arachnoiditis. Syrinx formation was unaltered. As the arachnoiditis did not significantly obstruct tracer flow it was concluded that the important effect of the arachnoiditis was localised compliance change preferentially diverting CSF into the SC and syrinxes[14], although the experiments did not rule out a mechanism based on tethering, nor did they investigate an effect on pulsatile flow. The study also does not rule out an important effect of flow obstruction when this exists (see e.g., Gottschalk et al., 2010). Others also propose that a Chiari-based reduction in SSS compliance concomitantly reduces spinal venous compliance, leading to diminished venous ISF absorption and subsequent syringomyelia (Bateman, 2004, 2010; Koyanagi and Houkin, 2010), albeit without fresh evidence.

Bertram et al. (2008) drew attention to tensile radial stress on cord tissue, arising transiently in the course of events associated with SSS wave propagation, as the crucial variable in a proposed mechanism for transverse tearing of cord tissue leading to syrinx formation. They

[14] It was earlier conjectured that the success of hindbrain decompression surgery for syringomyelia associated with Chiari malformation might be due to the increase in SSS compliance and concomitant reduction in SSS pulse pressure and perivascular flow (Stoodley et al., 1997).

showed examples where such stresses could be generated as a result of abnormally increased degrees of cord-to-dura linkage (tethering) in arachnoiditis. The computed stresses did not reach values that the cord was likely to find difficult to withstand. However, the simulations omitted other effects of subarachnoid scarring, including SSS stenosis, that would normally accompany cord tethering.

7.3 Where does syrinx fluid originate?

There have been many speculations (e.g., Levine, 2004; Greitz, 2006). Ball and Dayan (1972) established the PVS as a fluid conduit connecting the SSS with the syrinx. Water-soluble contrast media injected into the SSS accumulated in the PVS and syrinx; the PVS were dilated in histological sections, indicating a raised lumen pressure. In an animal model of post-traumatic syringomyelia (Brodbelt et al., 2003c), tracer studies using horseradish peroxidase (HRP) also sourced the syrinx fluid to the SSS. Tracer passed through the PVS, across the interstitial space and into the CC. No CSF path between the rat fourth ventricle and the CC was found, and the CC was observed to consist of isolated segments. Thus fluid could accumulate and syrinxes develop without CC action as a conduit. The flow was believed (Stoodley et al., 1996) to be driven by arterial pulsations, following an earlier suggestion (Rennels et al., 1985): "HRP influx [via PVS] results from a convective process which is facilitated by the pulsations of penetrating … arterioles."

Further evidence for the arterial-pulsation idea was provided by a study (Stoodley et al., 1997) on sheep: tracer movement from the SSS to the CC was abolished when the SC arterial pulsation was reduced (by partial vertebral artery ligation) while maintaining mean arterial pressure. When SC cavities were induced in rats by kaolin injection into the SSS (Stoodley et al., 1999), CSF took the same flow path into the syrinxes as into the CC, the syrinxes being simply dilated segments of the CC. However, CSF made its way into these syrinxes even when the surrounding tissue was visibly compressed, presumably due to raised lumen pressure. The kaolin also caused a SSS blockage, which, it was speculated, may induce elevated SSS pressure pulsation of cardiac frequency at rostral locations. Similar observations were made when non-CC syrinxes were created using an excitotoxic amino acid (Stoodley et al., 2000; Yang et al., 2001; Brodbelt et al., 2003b). These extra-canalicular syrinxes enlarged when a subarachnoid block due to arachnoiditis was present. In fact, CSF flowed preferentially into the syrinx, ahead of perivascular flow into the rostral portions of the SC (Brodbelt et al., 2003a). A more recent animal study from the same group demonstrated extra-canalicular syrinx fluid egress by tracking HRP reaction product in adjacent grey and white matter and around the central canal and perivascular spaces (Wong et al., 2012).

However, at this time, the alternative view, that syrinx fluid stems from capillary filtration, cannot be ruled out. Greitz (2006) and co-workers hypothesised that syringomyelia develops in the distended cord by accumulation of ISF derived from blood plasma, rather than from CSF[15]. Others have also argued that syrinx fluid differs in composition from CSF sufficiently that it is unlikely to be drawn from it (Levine, 2004), albeit without putting forward new evidence.

---

[15] Greitz et al. further argued that the pressure of the syrinx would then exert a compressive force on the venous outflow network which would increase venous resistance and increase arterial and capillary pressure, thereby reinforcing the pressure gradient driving the extracellular flow into the syrinx and making the mechanism self-sustaining. However, this step is separate from the basic premise of syrinx fluid from blood plasma via ISF.

7.4 Why are syrinxes few and large?

Arguably this question is ripe for engineering investigation, there having been so far little contribution from physical scientists. There are scarce reports of multiple cord syrinxes (Enomoto et al., 1984; Wester et al., 1989; Hamada et al., 1990; Hinokuma et al., 1992; Milhorat et al., 1995; George and Higginbotham, 2011) and septated syrinxes (Lederhaus et al., 1988; Davis and Symon, 1989; Pillay et al., 1991; George and Higginbotham, 2011), and Do-Dai et al. (2010) recently stated that "the syrinx fluid spaces are contiguous despite the loculated appearance"[16], a description also used by others (Roosen et al., 1988; Davis and Symon, 1989; Pillay et al., 1991; George and Higginbotham, 2011). In principle, a given macroscopic syrinx may have originated from just one microscopic syrinx, or from a large number of microscopic cavities, with all others having been competitively ousted. The observations of Fischbein et al. (1999, 2000) suggest that a local oedematous state may precede syrinx development, but it remains unknown how and why the conditions that provoked the original oedema will ultimately resolve in typically a single large syrinx. If oedema is indeed a precursor of syringomyelia, it would seem that some as-yet unidentified instability favours the further growth of a small cavity at the expense of its neighbours once it passes some threshold (of size or other property)[17].

7.5 Why are syrinxes localised to sites of SSS abnormality?

Any site of SSS property change will cause pressure wave reflections. At a partial blockage these reflections will increase the pressure. In linear theory, the maximum possible is local doubling of the pressure, but the wave will already have been attenuated in transit from its site of inception, and the localisation is not that sharp (Bertram et al., 2005). Carpenter et al. invoked reflection of nonlinearly steepened waves as a mechanism which pressure could increase very locally by more than a factor of two, but this was ultimately judged quantitatively infeasible. SSS stenosis may produce a Venturi effect as Greitz suggested, but the effect is likely to be small and overshadowed by larger pressure changes associated with overcoming flow resistance and accelerating fluid. A stenosis also causes transient 'pressure dissociation', reciprocal (and reciprocating) swings in SSS pressure and cord deformation at the two ends of a co-located syrinx, but on average these balance out, unless a further nonlinear action occurs. An association of syringomyelia with SC tethering has also long been noted (Klekamp, 2009). Bertram et al.'s (2008) modelling demonstrated a possible mechanical basis for this, as discussed above in §7.2.

Wave-induced fluid exchange across the pial membrane may play a role in syrinx filling. Elliott investigated this conjecture with a pair of 1-d analytical models based on elastic tube theory coupled with Darcy's law for either perivascular or interstitial flow (Elliott, 2012). Results showed that transpial flux serves as a mechanism for damping CSF pressure pulse waves by alleviating the contained hoop stress. The timescale ratio over which viscous and inertial forces compete was determined explicitly, which predicts that dilated PVS, SSS flow obstructions, and a stiffer and thicker pial membrane—all associated with syringomyelia—

---

[16] Also the predominant experience of neurosurgeon A. Aschoff (personal communication to CDB, July 2011).

[17] The mechanism might involve the law of Laplace as it applies to thin-walled pressure vessels; more wall stress is induced for a given pressure and wall thickness as the radius increases. The parenchymal surface of a small cavity is not a thin wall, but the mechanical principle favouring further enlargement of the larger of two small cavities still holds.

will increase transpial flux and retard wave travel.

7.6 What causes an existing syrinx to grow?

Syrinxes tend to be co-located with SSS stenosis, whether from post-traumatic scarring or from Chiari malformation. Although a juxtaposed stenosis causes considerable SSS pressure dissociation, this appears to augment the syrinx fluid motions caused by adjacent SSS pressure wave transit to only a minor extent. Cord tearing stress induced by syrinx fluid motion does not seem likely to exceed the magnitude of SSS pressure transients, but can reach 40% of their magnitude, while that induced at the cranial end of a syrinx with co-located severe SSS stenosis by periodic (sinusoidal) excitation at cardiac frequencies (Bertram, 2010) can exceed 80% of excitation amplitude. Coughing can cause transients of up to 10 kPa (75 mmHg; Williams, 1976), which is twice the measured transverse tensile stiffness of cord tissue (Ozawa et al., 2004). Together these figures suggest that syrinx lengthening by fluid-slosh is feasible.

In competition with any lengthening mechanism though is the extent to which the syrinx can be stabilised. Stoodley and colleagues recently demonstrated in a rat model of post-traumatic syringomyelia that after the initial syrinx formation there is a proliferation of cells around the syrinx that are involved in (glial) scar formation, which they proposed may act to limit further syrinx enlargement (Tu et al., 2010; Fehlings and Austin, 2011; Tu et al., 2011). Using a sheep model to demonstrate syrinx fluid outflow (Wong et al., 2012), they have also revived the question of whether syrinx growth could be due to a small imbalance between substantial in- and outflows.

7.7 How can syrinx pressure exceed CSF pressure in the SSS?

Some syrinxes appear on MRI to distend the cord locally into the SSS, and a significant proportion of syrinxes in the CC (22%) and parenchyma (37%) have been shown to rupture through the pia (Milhorat et al., 1995); this is persuasive evidence of elevated syrinx pressure. However, SSS pressure is itself above atmospheric, so that surgical opening of first the SSS and then of a syrinx can lead to fluid spurting in both instances, without any excess syrinx pressure (e.g., Brodbelt and Stoodley, 2003, fig. 3B). The true situation remains controversial.

The question also relates to how a pre-syrinx oedema might arise. Greitz (2006) suggested that syrinx fluid came via ISF from a relatively high-pressure source, the intra-cord capillaries, not the SSS. All other suggestions depend on a valve effect. Williams postulated one in the upper CC plus hindbrain hernia, but most syrinxes are non-communicating, either because they are extra-canalicular or because the CC has become discontinuous. Ellertsson and Greitz (1970) measured intra-syrinx pressure under resting conditions and found it to be greater than SSS pressure but with lower pulse amplitude. During Queckenstedt[18] and Valsalva manoeuvres the syrinx pressure rose later and persisted longer than the SSS pressure. This suggested to them that there exists a pathway between the CSF and syrinx spaces other than the CC, and that a transiently favourable pressure gradient at the syrinx 'inlet' in combination with defective syrinx drainage accounted for the persistently raised syrinx pressure. However this much does not amount to a full mechanism for elevated syrinx mean pressure. Furthermore, these percutaneous measurements may have interfered with the intra-syrinx

[18] The jugular veins are manually compressed to raise venous pressure and intracranial CSF pressure. If lumbar CSF pressure (measured by lumbar puncture) remains almost unaltered, or its rise is delayed, there is a SSS blockage.

pressure that they sought to quantify.

Engineering contributions have identified two functional valves. One, at the level of the PVS (Bilston et al., 2010), relies on out-of-phase arrival of arterial and SSS pressure pulses. The other is the result of flexible SSS stenosis (Bertram, 2010; Martin et al., 2010).

7.7.1 PVS valving (Bilston)

The resistance of a PVS enclosing an artery is influenced by the distension of that vessel, which varies with the cardiac pulse. Bilston et al. modelled a PVS as an annular cylinder, applying a prescribed (axisymmetric) long-wavelength deformation based on human arterial measurements to the inner surface (Bilston et al., 2007; Bilston et al., 2010). SSS pulse pressure computed from human SSS flow-rate measurements (Bilston et al., 2006) was applied to the SSS end of the PVS, and zero pressure at the other end. Phase difference between the two pulses caused a net flux in one direction, with maximal PVS inflow corresponding to the pulses being out of phase, making it easy for fluid to enter the cord but difficult to leave. Bilston et al. (2010) hypothesized that interruptions to the local blood supply such as scar tissue could lead to such phase differences.

Although only a feasibility study, the model's usefulness is limited by the fact that the greater part of the cerebrospinal system was omitted. Furthermore, with the intra-cord pressure fixed at zero the effect of PVS flow on cord/syrinx pressure could not be ascertained.

Elliott et al. (2011) addressed these concerns with lumped-parameter models of the whole cerebrospinal system. Both models had compartments representing (i) the SC, (ii) the SSS, (iii) the venous bed of the SC, (iv) the venous bed of the SSS and epidural space, and (v) a vascular pressure source, and the more detailed model included (vi) ventricles and (vii) the brain. CSF could be exchanged between the SC (interstitium) and SSS via perivascular conductance at the pia. The change in volume of the SSS and SC compartments in response to a pressure difference across the pia was modelled by a compliance at that boundary. Similar compliances allowed for collapse of the SC venous bed and displacement of fluid in the epidural space. The vascular source compartment provided a sinusoidal driving pressure to the SC and SSS via further compliant interfaces.

When pial conductance was varied periodically with a phase lag relative to SSS vascular driving pressure, the eventual mean pressures in the SC and SSS differed. The excess SC pressure was maximally positive if pial conductance and vascular pressure were completely out of phase, but approached zero (mean and pulse amplitude) in the limit of zero compliance of the SC venous bed; i.e., the pressure gradient driving fluid into the cord also constricts the cord so the two effects cancel, unless the SC venous fluid can be independently displaced. Thus for the mechanism to operate, the SC must have volume compliance due to displacement of blood from the SC venous bed. This requirement is quite restrictive as the SC venous volume, although as yet unmeasured, is unlikely to be substantial.

The feature of Elliott et al.'s (2011) models[19] that is most difficult to assess is the vascular system. Its functional division into pressure source and volume compliance does not lend itself readily to physiological estimates of the associated compliance and pulsation parameters. Another limitation is the use of constant rather than volume-dependent

[19] A second, more detailed model was used to investigate the role that phasic pumping might play in post-traumatic syringomyelia (subarachnoid scar tissue, syrinx) and standard surgical treatments (syringo-subarachnoid shunt, subarachnoid bypass).

compliances; the overall compliance of the SSS is strongly volume-dependent (Marmarou et al., 1975). Phasic PVS pumping only addresses the question posed in the section title; if anything it would seem that the required phase differences, and therefore syrinxes, were most likely to develop at the caudal end of the spinal canal, rather than in the neck and thorax.

To assess the possible phase differences that might exist between CSF and arterial pulsations along the spinal cord, Martin et al. (2012) constructed a coupled model of the cardiovascular and CSF system in the spine including blood flow along the SC. They found that the relative arrival time of CSF and arterial pulsations along the SC were strongly impacted by CSF system compliance and vascular anatomy. This model was also used to predict axial distribution of perivascular flow to the SC based on the results of Bilston et al. (2010) for the PVS of a single arteriole. As with the study of Elliott et al. (2011) the lumbar spine was found to have greater perivascular flow than other regions.

7.7.2 Flexible SSS stenosis (Bertram/Martin)

This putative mechanism for elevated syrinx pressure, which has yet to be fully investigated, does not depend on phase. A flexible SSS stenosis elevates mean SSS pressure caudal to itself (Bertram, 2010; Martin et al., 2010). Bertram showed that in the absence of syrinx inflow, and for a stenosis located at syrinx mid-point, simulated mean syrinx pressure was much closer to SSS pressure rostral to the stenosis (Bertram, 2010, fig. 9b). The excess of SSS pressure caudal to the stenosis would appear to favour inflow to the syrinx, whether via the PVS or filtered through cord tissue, leading to a syrinx pressure above the mean CSF pressure rostral to the syrinx. The same might apply to a syrinx caudal to a site of SSS stenosis, although this situation has yet to be tested. Following subarachnoid scarring in the thoracic region, syrinxes typically extend cervically (Brodbelt and Stoodley, 2003; Klekamp, 2009), whereas cervical syrinxes due to scarring (Klekamp, 2009), and Chiari-based syrinxes, are typically slightly lower down the cord than the scar or site of tonsillar herniation; this mechanism would suggest that only syrinxes located lower down would be expected to have high pressure. This in turn might explain the lack of unanimity in the literature about elevated syrinx pressure.

7.8 Why does syringomyelia develop slowly?

Computer models (Bertram et al., 2005; Bertram et al., 2008; Elliott et al., 2009; Bertram, 2010; Elliott et al., 2011) under various scenarios of system excitation (frequency content, transient/repetitive, cranial/abdominal) and pathology (syrinx presence, subarachnoid stenosis or tethering) have uniformly failed to predict unwontedly large fluid pressures or cord-tissue tearing stresses. This is perhaps not surprising; syringomyelia is a rare disease[20] that takes years to develop. Thus it is possible that the causal mechanism will lurk below any anticipated threshold for acute or immediate damage in response to stimuli simulating physiological events such as the arterial pressure pulse or cough-related transients.

However, such thresholds may themselves be lower than most of what Table 1 suggests. In elegant experiments, Ozawa et al. (2004) measured the resistance to transverse pulling of

---

[20] Prevalence estimates range from 0.84 to 8.5 cases per 10,000 (Brewis et al., 1966; Speer et al., 2003). In the European Union a rare disease is defined to have a prevalence of less than 5 per 10,000 (European Commission, 2004); in the U. S. A. a prevalence of less than 200,000 individuals (equating to less than 7 per 10,000 in 2011) qualifies as a rare disease (Rare Diseases Act of 2002, Public Law 107-280, 116 Stat. 1987).

segments of rabbit SC with intact pia mater, then separately measured the properties of the pia. By comparison of the two datasets they extracted a figure for the transverse tensile stiffness of cord tissue itself: 5±2 kPa. This is much lower than most solids, and recalls words quoted by Carpenter et al. (2003) about the custard-like consistency of the material. In combination with an unlucky conjunction of circumstances, bringing about (e.g.) a system resonance, it is then conceivable that the physical circumstances needed for a cavity to develop, to grow, and to contain fluid at elevated pressure, lie within the remit of the mechanisms that engineers are now investigating.

8 Conclusion and outlook

The tools that engineers bring to bear on the investigation of syringomyelia, whether analysis, or physical or numerical modelling, inevitably drastically oversimplify the multi-scale complexity of the biological situation. They also rest on the presumption, certainly not proven, that the condition is largely if not completely a consequence of mechanical factors rather than cellular biology. This is a rather strong assumption, encouraged by those neurosurgeons who sought the assistance of bioengineers originally, and makes syringomyelia almost uniquely suited to biomechanical investigation. Nevertheless, it may still ultimately prove that the premise was mistaken, and that both the origin and the cure will reside in fields far from engineering. The engineer does well to keep this in mind and remain humble.

However, simplification can also be an advantage if it reduces a situation in which cause and effect cannot be discerned to a comprehensible model. We have reviewed here the mechanical hypotheses for syrinx formation and expansion from neurosurgery and engineering. In doing so much has been established about the cerebrospinal physiology. We know that the flow of CSF in the SSS and of the fluid in fully-expanded syrinxes is inertia-dominated. Excitation from short pressure transients, such as from a cough or a sneeze, will generate pressure waves that impose stress on the cord tissue. This is especially true at pathological sites, where an impinging hindbrain or post-traumatic scar tissue acts to reflect and/or refract the incident waves due to local changes in compliance, flow resistance and cord tethering. The mechanics are timescale-dependent. Short-lived pressure waves do not induce much SSS fluid movement, unlike the slower systolic perturbations that are responsible for the reciprocating SSS flow, but are relatively efficient in provoking syrinx fluid motion.

Regarding pathogenesis hypotheses, elastic jumps, perivascular peristalsis and substantial Venturi effects are quantitatively unlikely. Our present state of knowledge suggests that syrinx fluid derives from either ISF, flowing down a pressure gradient, or CSF, being pumped uphill. For the latter, two systolic valve mechanisms have been identified: (i) a PVS valve that depends on the phasing of the CSF and arterial pulses, (ii) a cyclic pressure dissociation about a flexible SSS stenosis with an underlying syrinx. Williams' slosh mechanism for syrinx expansion remains feasible.

The above insights are gleaned from physical and mathematical models, with the latter subdividing into lumped-parameter models and continuum models. One of the more robust model validators is the pulse wave speed, which can be measured *in vivo* and on the bench, thus favouring the continuum approach. To predict the correct wave speed the model must have a functionally realistic system compliance. Both analytical and numerical solution methods have been used in what are mostly idealized models. More data on the distribution

of SSS compliance and the extent of wave propagation and reflection *in vivo* are sorely needed.

The most significant ongoing challenges to the engineer are measuring the *in-situ* constitutive properties of the spinal tissues and structures, and the multi-scale nature of the problem. The first is a challenge to the ingenuity of biomechanics experimenters. Regarding the second, the anatomical length scales span six or seven orders of magnitude, and the pathophysiological time-scales are even wider. This poses extreme demands of a numerical model; thus, there is some appeal for asymptotic methods.

There is an increasing trend for patient-specific modelling, driven largely by the ever-higher resolution of MR scanners and new MR measurement sequences. While this promises practical benefits to the surgeon, the increasing level of detail makes the mechanics more difficult to understand. For this reason highly idealized models will continue to serve an important role in elucidating the fundamental mechanics upon which more anatomically realistic models operate.

Conflict of interest statement

The authors have no conflict of interest that would influence the content of this manuscript.

Acknowledgements

CDB and NSJE would like to thank Laboratoire d'Hydrodynamique, Ecole Polytechnique, France, and the School of Mathematics, University of Manchester, U.K., respectively, for hosting them as honorary visitors during this paper's preparation. NSJE acknowledges the support of the Australian Research Council through project DP0559408 and the WA State Centre of Excellence in eMedicine. BAM acknowledges support from the Swiss National Science Foundation grant no. 205321_132695/1, and the Hemodynamics and Cardiovascular Technology Laboratory, Ecole Polytechnique Fédérale de Lausanne, Switzerland, where he was employed during this paper's preparation. All authors thank medical illustrator Beth Croce for service beyond duty in the production of Figure 2.

List of table captions

Table 1. Spinal cord tissues: experimental measurements of elasticity. Symbols: Young's modulus (E), shear modulus (G), stress (σ), strain (ε), applied force (F), Poisson's ratio (ν).

List of figure captions

Fig. 1. T2-weighted saggital MR images showing syrinxes in association with (a,b) Chiari malformation, and (c) spinal injury. (a) In this 37-year-old patient who presented with headache the cerebellar tonsil (*) lies low in the foramen magnum but CSF (white on this image) is seen around the tonsil. A prominent central canal (arrow head), or early syrinx, is seen. At this time analgesia alone controlled the symptoms. (b) Four years later the patient developed hand weakness and arm pain. The repeat MRI shows the cerebellar tonsil (*) with no CSF surrounding and a new syrinx (arrow head) and cord oedema rostral and caudal to the syrinx. (c) MRI of a patient following a significant spinal cord injury. The site of a bone graft used to stabilize and repair the vertebral column is shown (X). The patient developed worsening pain and motor function. The syrinx that has developed is shown (arrowhead).

Fig. 2. Gross anatomy of the spinal cord featuring the meninges. (a) depicts the cord in its location within the vertebrae and (b) is a cross-sectional view in which the cord is cut at a level slightly higher than the vertebra.

Fig. 3. Pathways of CSF flow. Reproduced with permission from Netter (1953).

Fig. 4. Schematic diagram showing the fluid spaces on either side of the cranial pial membrane. The situation of the spinal pial membrane and surrounding fluids is thought to be similar although this is not known for certain. Slightly different notation to the text is used here: A = arachnoid mater, SAS = subarachnoid space, PAS = periarterial space, PF = perforated, CAPS = capillary. Note the pia-like sheaths around both blood vessels, which is lost in the cortex in the case of the vein, their perforations and the subpial fluid space along the cortex surface. Not shown are the leaky gap junctions in the pial membrane that also permit fluid to be exchanged between the SAS and the PVS. Reproduced with permission from Zhang et al. (1990), figure 10.

Fig. 5. Pressure dissociation following (a) a cough and (b) a Valsalva manoeuvre. See text for detailed explanation. Panels (a) and (b) reproduced with permission from Williams (1980), figures 1 and 2 respectively.

Table 1. Spinal cord tissues: experimental measurements of elasticity. Symbols: Young's modulus (E), shear modulus (G), stress (σ), strain (ε), applied force (F), Poisson's ratio (ν).

tissue	species	E (kPa)	test direction		test mode	ref.
cervical spinal cord	rabbit	5 ±2	transverse	width 5 ±0.5 mm	1D-tension	(Ozawa et al., 2004)
spinal cord	human	89 @ $1s^{-1}$ & 10 s^{-1}	axial		1D-tension	(Mazuchowski and Thibault, 2003)
thoracic spinal cord	dog	16.8 (low σ), 11.9 (high σ)[i]	axial		1D-tension	(Tunturi, 1978)
lumbar spinal cord	rat	6.63 ± 0.75		f = 1 Hz, 10 cycles	cylindrical indentor	(Saxena et al., 2009)
cord gray matter	cow cervical	1660 ±160 @ 0.05 s^{-1}	axial	ν_P = 0.4	1D-tension	(Ichihara et al., 2001)
cord gray matter	rabbit cervical	3			pipette aspiration	(Ozawa et al., 2001)
cord white matter	rabbit cervical	3.5			pipette aspiration	(Ozawa et al., 2001)
cord white matter	cow cervical	940 ±130 @ 0.05 s^{-1}	axial	ν_P = 0.4	1D-tension	(Ichihara et al., 2001)
cord white matter	guinea pig abd.	injury at $\sigma_{von\ Mises}$ ~ 2	transverse	0.05 mm/s	compression	(Ouyang et al., 2008)
cervical cord + pia	human	520–1880 @ 0.04–0.24 s^{-1}	axial		1D-tension	(Bilston and Thibault, 1996)
spinal cord + pia	human	1400 @ $1s^{-1}$ & 10 s^{-1}	axial		1D-tension	(Mazuchowski and Thiba

						ult, 2003)
spinal cord + pia	cow	1190 @ 0.24 s^{-1}	axial	1950 after 72 hours	1D-tension	(Oakland et al., 2006)
lumbar cord + pia	cats *in vivo*	230 @ 0.003–0.012 s^{-1}	axial	n = 9	1D-tension	(Chang and Hung, 1988)
lumbar cord + pia	cats *in vivo*	220–295 @ 0.002 s^{-1}	axial	$\varepsilon < 0.05$ n = 17	1D-tension	(Hung et al., 1981)
lumbar cord + pia	puppies *in vivo*	265 @ 0.0021–0.0035 s^{-1}	axial		1D-tension	(Hung and Chang, 1981)
lumbar cord + pia	puppies *in vivo*	215–295 @ 0.02 mm s^{-1}	axial	$\varepsilon < 0.05$ n = 10	1D-tension	(Chang et al., 1981)[i][i]
thorac. cord[iii] + pia	cats *in vivo*	1–2 (low ε), 10 (high ε)	transverse	0.002 mm/s	compression	(Hung et al., 1982)
cervical pia mater	rabbit	2300	circumferential	thickness 12±3 µm	1D-tension	(Ozawa et al., 2004)
dura mater	human	172 MPa lumbar, 129 MPa cervical	longitudinal		1D-tension	(Tencer et al., 1985)
lumbar dura mater	human	65–103 MPa 4–8 MPa	longitudinal circumferential		1D-tension	(Runza et al., 1999)
lumbar dura mater	human	26.1–62 MPa[iv] 4.0–14.3 MPa	longitudinal transverse		1D-tension	(Zarzur, 1996)
lumbar dura mater	human	F/ε = 15–27 kPa[v] F/ε = 0.8–3.8 kPa	longitudinal transverse		1D-tension	(Patin et al., 1993)
lumbar dura mater	cow	27–80 MPa	longitudinal		1D-tension	(Runza et al., 1999)
spinal dura mater	cow	k = 1.2 MPa[vi] k = 138 MPa	longitudinal circumferential		1D-tension	(Wilcox et al., 2003)

thoraco-lumbar dura	dog	0.4 MPa (low σ), 46 MPa (high σ)	longitudinal	$\varepsilon = 0.14$ $\varepsilon = 0.18$	1D-tension	(Tunturi, 1977)
spinal dura mater	cat *in vivo*	2 MPa	longitudinal	$\varepsilon < 0.06$ $n = 1$	1D-tension	(Chang and Hung, 1988)
spinal dura mater	rat	$G = 1.2$ MPa	longitudinal	.0014 s^{-1} 19.4 s^{-1}	1D-tension	(Maikos et al., 2008)

[i] The decreasing stiffness was attributed to viscous flow, and was entirely different from the increasing stiffness of specimens of cord + pia + denticulate ligaments.

[ii] These results are a re-reporting of those given by Hung and Chang (1981); the two rows of the table refer to the same data.

[iii] The paper does not mention whether the pia was present or not (Hung et al., 1982). Based on the date, and the difficulty of handling pia-less cord, it is assumed that the pia was intact.

[iv] These are not the elastic modulus figures given by Zarzur (1996; Table 2), which are incorrect. Recalculation based on the other data supplied gives much larger figures summarised here.

[v] These figures are not comparable with those in the rest of the column, because "stiffness" is here simply force/strain, without consideration of cross-sectional area.

[vi] k is an elastic constant, but not equal to E; the relative values indicate the extent of anisotropy (qualitatively opposite to that measured by Runza et al., 1999).

References

The Visible Human Project®. U.S. National Library of Medicine.
2002. Rare Diseases Act of 2002, Public Law 107-280, 116 Stat. 1987.
2004. Useful information on rare diseases from an EU perspectives, Meeting of the Network of Competent Authorities for Health Information and Knowledge. European Commission, Luxembourg; .
2006a. Merriam-Webster's Medical Dictionary, 2nd ed. Merriam-Webster, Springfield, MA.
2006b. Stedman's Medical Dictionary, 28th ed. Lippincott Williams and Wilkins, Philadelphia.
Ball, M.J., Dayan, A.D., 1972. Pathogenesis of syringomyelia. The Lancet 2, 799–801.
Barnett, H.J.M., 1973. Syringomyelia associated with spinal arachnoiditis, in: Barnett, H.J.M., Foster, J.B., Hudgson, P. (Eds.), Syringomyelia. W. B. Saunders, London, pp. 220–244.
Barshes, N., Demopoulos, A., Engelhard, H.H., 2005. Anatomy and physiology of the leptomeninges and CSF space, in: Abrey, L.E., Chamberlain, M.C., Engelhard, H.H. (Eds.), Leptomeningeal Metastases. Springer Science+Business Media, Inc., New York, pp. 1–16.
Bastian, H.C., 1867. On a case of concussion-lesion with extensive secondary degeneration of the spinal cord, followed by general muscular atrophy. Medico-Chirurgical Transactions 50, 499–542.
Bateman, G.A., 2004. The role of altered impedance in the pathophysiology of normal pressure hydrocephalus, Alzheimer's disease and syringomyelia. Medical Hypotheses 63, 980–985.
Bateman, G.A., 2010. The correlations between a proposed pathogenesis of syringomyelia and normal pressure hydrocephalus. Neurosurgical Review 33, 505–506.
Battal, B., Kocaoglu, M., Bulakbasi, N., Husmen, G., Tuba Sanal, H., Tayfun, C., 2011. Cerebrospinal fluid flow imaging by using phase-contrast MR technique. The British Journal of Radiology 84, 758–765.
Batzdorf, U., Klekamp, J., Johnson, J.P., 1998. A critical appraisal of syrinx cavity shunting procedures. Journal of Neurosurgery 89, 382–388.
Berkouk, K., Carpenter, P.W., Lucey, A.D., 2003. Pressure wave propagation in fluid-filled co-axial elastic tubes, Part 1: basic theory. Journal of Biomechanical Engineering 125, 852–856.
Bertram, C.D., 2009. A numerical investigation of waves propagating in the spinal cord and subarachnoid space in the presence of a syrinx. Journal of Fluids and Structures 25, 1189–1205.
Bertram, C.D., 2010. Evaluation by fluid/structure-interaction spinal-cord simulation of the effects of subarachnoid-space stenosis on an adjacent syrinx. Journal of Biomechanical Engineering 132, 061009-061001–061015.
Bertram, C.D., Bilston, L.E., Stoodley, M.A., 2008. Tensile radial stress in the spinal cord related to arachnoiditis or tethering: a numerical model. Medical and Biological Engineering and Computing 46, 701–707.
Bertram, C.D., Brodbelt, A.R., Stoodley, M.A., 2005. The origins of syringomyelia: numerical models of fluid/structure interactions in the spinal cord. Journal of Biomechanical Engineering 127, 1099–1109.
Beulen, B.W.A.M.M., Rutten, M.C.M., van de Vosse, F.N., 2009. A time-periodic approach for fluid-structure interaction in distensible vessels. Journal of Fluids and Structures 25, 954–966.
Bilston, L.E., Fletcher, D.F., Brodbelt, A.R., Stoodley, M.A., 2003. Arterial pulsation-driven cerebrospinal fluid motion in the perivascular space: a computational model. Computer Methods in Biomechanics and Biomedical Engineering 6, 235–241.
Bilston, L.E., Fletcher, D.F., Stoodley, M.A., 2006. Focal spinal arachnoiditis increases subarachnoid space pressure: a computational study. Clinical Biomechanics 21, 579–584.

Bilston, L.E., Fletcher, D.F., Stoodley, M.A., 2007. Effect of phase differences between cardiac and CSF pulse on perivascular flow - a computational model with relevance to syringomyelia. British Journal of Neurosurgery 21, 430.
Bilston, L.E., Stoodley, M.A., Fletcher, D.F., 2010. The influence of the relative timing of arterial and subarachnoid space pulse waves on spinal perivascular cerebrospinal fluid flow as a possible factor in syrinx developments. Journal of Neurosurgery 112, 808–813.
Bilston, L.E., Thibault, L.E., 1996. The mechanical properties of the human cervical spinal cord in vitro. Annals of Biomedical Engineering 24, 67–74.
Bloomfield, I.G., Johnson, I.H., Bilston, L.E., 1998. Effects of proteins, blood cells and glucose on the viscosity of cerebrospinal fluid. Pediatric Neurosurgery 28, 246–251.
Boman, K., Iivanainen, M., 1967. Prognosis of syringomyelia. Acta Neurologica Scandinavica 43, 61–68.
Bradbury, M., 1993. Anatomy and physiology of CSF, Hydrocephalus. Oxford University Press, pp. 19–47.
Brewis, M., Poskanzer, D.C., Rolland, C., Miller, H., 1966. Neurological disease in an English city. Acta Neurologica Scandinavica 42, 1–89.
Brodbelt, A., Stoodley, M., 2007. CSF pathways: a review. British Journal of Neurosurgery 21, 510–520.
Brodbelt, A., Stoodley, M., Watling, A., Tu, J., Jones, N., 2003a. Fluid flow in an animal model of post-traumatic syringomyelia. European Spine Journal 12, 300–306.
Brodbelt, A.R., Stoodley, M.A., 2003. Post-traumatic syringomyelia: a review. Journal of Clinical Neuroscience 10, 401–408.
Brodbelt, A.R., Stoodley, M.A., Watling, A.M., Rogan, C., Tu, J., Brown, C.J., Burke, S., Jones, N.R., 2003b. The role of excitotoxic injury in post-traumatic syringomyelia. Journal of Neurotrauma 20, 883–893.
Brodbelt, A.R., Stoodley, M.A., Watling, A.M., Tu, J., Burke, S., Jones, N.R., 2003c. Altered subarachnoid space compliance and fluid flow in an animal model of posttraumatic syringomyelia. Spine 28, E413–E419.
Brugières, P., Idy-Peretti, I., Iffenecker, C., Parker, F., Jolivet, O., Hurth, M., Gaston, A., Bittoun, J., 2000. CSF flow measurement in syringomyelia. American Journal of Neuroradiology 21, 1785–1792.
Brunner, J.C., 1700. Hydrocephalo, sire hydrope capitis, in: Bonneti, T. (Ed.), Sepulchretum, Miscell. Nat. Curios. III Dec. Ann. I 1688, Ed II, Lib I ed. Cramer & Perachon, Genf, p. 394.
Bunck, A.C., Kröger, J.-R., Jüttner, A., Brentrup, A., Fiedler, B., Schaarschmidt, F., Crelier, G.R., Schwindt, W., Heindel, W., Niederstadt, T., Maintz, D., 2011. Magnetic resonance 4D flow characteristics of cerebrospinal fluid at the craniocervical junction and the cervical spinal canal. European Radiology 21, 1788–1796.
Carpenter, P.W., Berkouk, K., Lucey, A.D., 1999. A theoretical model of pressure wave propagation in the human spinal CSF system. Engineering Mechanics 6, 213–228.
Carpenter, P.W., Berkouk, K., Lucey, A.D., 2003. Pressure wave propagation in fluid-filled co-axial elastic tubes, Part 2: mechanisms for the pathogenesis of syringomyelia. Journal of Biomechanical Engineering 125, 857–863.
Chang, G.L., Hung, T.K., 1988. An in-vivo measurement and analysis of viscoelastic properties of the spinal cord of cats. Journal of Biomechanical Engineering 110, 115–122.
Chang, G.L., Hung, T.K., Bleyaert, A., Jannetta, P.J., 1981. Stress--strain measurement of the spinal cord of puppies and their neurological evaluation. Journal of Trauma 21, 807–810.
Chang, H.S., Nakagawa, H., 2003. Hypothesis on the pathophysiology of syringomyelia based on simulation of cerebrospinal fluid dynamics. Journal of Neurology, Neurosurgery and Psychiatry 74, 344–347.
Chang, H.S., Nakagawa, H., 2004. Theoretical analysis of the pathophysiology of syringomyelia associated with adhesive arachnoiditis. Journal of Neurology, Neurosurgery and Psychiatry

75, 754–757.
Charcot, J.M., Joffroy, A., 1869. Deux cas d'atrophie musculaire progressive avec lésions de la substance grise et des faisceaux antérolatéraux de la moelle épinière. Archives de Physiologie Normale et Pathologique 2, 354–367.
Chouly, F., Van Hirtum, A., Lagrée, P.-Y., Pelorson, X., Payan, Y., 2008. Numerical and experimental study of expiratory flow in the case of major upper airway obstructions with fluid–structure interaction. Journal of Fluids and Structures 24, 250–269.
Cirovic, S., 2009. A coaxial tube model of the cerebrospinal fluid pulse propagation in the spinal column. Journal of Biomechanical Engineering 131, 021008-021001–021009.
Cirovic, S., Kim, M., 2012. A one-dimensional model of the spinal cerebrospinal-fluid compartment. Journal of Biomechanical Engineering 134, 021005-021001–021010.
Clausen, J.R., Reasor, D.A., Aidun, C.K., 2011. The rheology and microstructure of concentrated non-colloidal suspensions of deformable capsules. Journal of Fluid Mechanics 685, 202–234.
Cloyd, M.W., Low, F.N., 1974. Scanning electron microscopy of the subarachnoid space in the dog. I. Spinal cord levels. Journal of Comparative Neurology 153, 325–367.
Crossman, A., Neary, D., 2001. Neuroanatomy: An Illustrated Colour Text. Churchill Livingstone.
Davis, C.H.G., Symon, L., 1989. Mechanisms and treatment in post-traumatic syringomyelia. British Journal of Neurosurgery 3, 669–674.
Do-Dai, D.D., Brooks, M.K., Goldkamp, A., Erbay, S., Bhadelia, R.A., 2010. Magnetic resonance imaging of intramedullary spinal cord lesions: a pictorial review. Current Problems in Diagnostic Radiology 39, 160–185.
Edgar, R., Quail, P., 1994. Progressive post-traumatic cystic and non-cystic myelopathy. British Journal of Neurosurgery 8, 7–22.
Ellertsson, A.B., Greitz, T., 1970. The distending force in the production of communicating syringomyelia. The Lancet 1, 1234.
Elliott, N.S.J., 2012. Syrinx fluid transport: modeling pressure-wave-induced flux across the spinal pial membrane. Journal of Biomechanical Engineering 134, 031006-031001–031009.
Elliott, N.S.J., Lockerby, D.A., Brodbelt, A.R., 2009. The pathogenesis of syringomyelia: a re-evaluation of the elastic-jump hypothesis. Journal of Biomechanical Engineering 131, 044503-044501–044506.
Elliott, N.S.J., Lockerby, D.A., Brodbelt, A.R., 2011. A lumped-parameter model of the cerebrospinal system for investigating arterial-driven flow in posttraumatic syringomyelia. Medical Engineering & Physics 33 874–882.
England, M.A., Wakeley, J.W., 2006. Color Atlas of the Brain and Spinal Cord: An Introduction to Normal Neuroanatomy. Mosby.
Enomoto, H., Shibata, T., Ito, A., Harada, T., Satake, T., 1984. Multiple hemangioblastomas accompanied by syringomyelia in the cerebellum and the spinal cord. Surgical Neurology 22, 197–203.
Fehlings, M.G., Austin, J.W., 2011. Editorial: Posttraumatic syringomyelia. Journal of Neurosurgery: Spine 14, 570–572.
Fischbein, N.J., Dillon, W.P., Cobbs, C., Weinstein, P.R., 1999. The "presyrinx" state: a reversible myelopathic condition that may precede syringomyelia. American Journal of Neuroradiology 20, 7–20.
Fischbein, N.J., Dillon, W.P., Cobbs, C., Weinstein, P.R., 2000. The "presyrinx" state: is there a reversible myelopathic condition that may precede syringomyelia? Neurosurgical Focus 8, 1–13.
Fricke, B., Andres, K.H., Von During, M., 2001. Nerve fibers innervating the cranial and spinal meninges: morphology of nerve fiber terminals and their structural integration. Microscopy Research and Technique 53, 96-105.
Gardner, W.J., 1965. Hydrodynamic mechanism of syringomyelia: its relationship to

myelocele. Journal of Neurology, Neurosurgery and Psychiatry 28, 247–259.
Gardner, W.J., Angel, J., 1959. The mechanism of syringomyelia and its surgical correction, Clinical Neurosurgery, Proceedings of the Congress of Neurological Surgeons, San Francisco, U.S.A., 1958. The Williams & Wilkins Company, Baltimore, pp. 131–140.
Gardner, W.J., Goodall, R.J., 1950. The surgical treatment of Arnold-Chiari malformation in adults: an explanation of its mechanism and importance of encephalography in diagnosis. Journal of Neurosurgery 7, 199–206.
George, T.M., Higginbotham, N.H., 2011. Defining the signs and symptoms of Chiari malformation type I with and without syringomyelia. Neurological Research 33, 240–246.
Gillies, G.T., Wilhelm, T.D., Humphrey, J.A.C., Fillmore, H.L., Holloway, K.L., Broaddus, W.C., 2002. A spinal cord surrogate with nanoscale porosity for in vitro simulations of restorative neurosurgical techniques. Nanotechnology 13.
Gottschalk, A., Schmitz, B., Mauer, U.M., Bornstedt, A., Steinhoff, S., Danz, B., Schlötzer, W., Rasche, V., 2010. Dynamic visualization of arachnoid adhesions in a patient with idiopathic syringomyelia using high-resolution cine magnetic resonance imaging at 3T. Journal of Magnetic Resonance Imaging 32, 218–222.
Gray, H., 1918. Anatomy of the Human Body. Lea & Febiger, Philadelphia.
Greitz, D., 1995. CSF-flow at the craniocervical junction: increased systolic and diastolic pressure gradients as the cause of cystic cord lesions, in: Kenéz, J. (Ed.), Imaging of the Craniocervical Junction. Edizione del Centauro, Udine Milano, pp. 19–23.
Greitz, D., 2006. Unravelling the riddle of syringomyelia. Neurosurgical Review 29, 251–264.
Greitz, D., Ericson, K., Flodmark, O., 1999. Pathogenesis and mechanics of spinal cord cysts – a new hypothesis based on magnetic resonance studies of cerebrospinal fluid dynamics. International Journal of Neuroradiology 5, 61–78.
Greitz, D., Flodmark, O., 2004. Modern concepts of syringohydromyelia. Rivista di Neuroradiologia 17, 360–361.
Greitz, D., Hannerz, J., 1996. A proposed model of cerebrospinal fluid circulation: Observations with radionuclide cisternography. American Journal of Neuroradiology 17, 431–438.
Grotberg, J.B., Jensen, O.E., 2004. Biofluid mechanics in flexible tubes. Annual Review of Fluid Mechanics 36, 121–147.
Gupta, S., Poulikakos, D., Kurtcuoglu, V., 2008. Analytical solution for pulsatile viscous flow in a straight elliptic annulus and application to the motion of the cerebrospinal fluid. Physics of Fluids 20, 093607-093601–093612.
Gupta, S., Soellinger, M., Boesiger, P., Poulikakos, D., Kurtcuoglu, V., 2009. Three-dimensional computational modeling of subject-specific cerebrospinal fluid flow in the subarachnoid space. Journal of Biomechanical Engineering 131, 021010-021011–021011.
Guyton, A.C., Hall, J.E., 2006. Textbook of Medical Physiology. Elsevier Saunders, Philadelphia.
Häckel, M., Beneš, V., Mohapl, M., 2001. Simultaneous cerebral and spinal fluid pressure recordings in surgical indications of the Chiari malformation without myelodysplasia. Acta Neurochirurgica 143, 909–918.
Hall, P., Turner, M., Aichinger, S., Bendick, P., Campbell, R., 1980. Experimental syringomyelia: the relationship between intraventricular and intrasyrinx pressures. Journal of Neurosurgery 52, 812–817.
Hamada, K., Sudoh, K., Fukaura, H., Yanagihara, T., Hamada, T., Tashiro, K., Isu, T., 1990. [An autopsy case of amyotrophic lateral sclerosis associated with cervical syringomyelia]. No To Shinkei 42, 527–531.
Harris, P.J., Hardwidge, C., 2010. A porous finite element model of the motion of the spinal cord, in: Constanda, C., Pérez, M.E. (Eds.), Integral Methods in Science and Engineering. Springer, pp. 193–201.
Heil, M., Hazel, A.L., 2011. Fluid-structure interaction in internal physiological flows. Annual Review of Fluid Mechanics 43, 141–162.

Heiss, J.D., Patronas, N., DeVroom, H.L., Shawker, T., Ennis, R., Kammerer, W., Eidsath, A., Talbot, T., Morris, J., Eskioglu, E., Oldfield, E.H., 1999. Elucidating the pathophysiology of syringomyelia. Journal of Neurosurgery 91, 553–562.
Hemley, S.J., Tu, J., Stoodley, M.A., 2009. Role of the blood-spinal cord barrier in posttraumatic syringomyelia. Journal of Neurosurgery: Spine 11, 696–704.
Henry-Feugeas, M.-C., Idy-Peretti, I., Baledent, O., Poncelet-Didon, A., Zannoli, G., Bittoun, J., Schouman-Claeys, E., 2000. Origin of subarachnoid cerebrospinal fluid pulsations: a phase-contrast MR analysis. Magnetic Resonance Imaging 18, 387–395.
Hentschel, S., Mardal, K.-A., Løvgren, A.E., Linge, S., Haughton, V., 2010. Characterization of cyclic CSF flow in the foramen magnum and upper cervical spinal canal with MR flow imaging and computational fluid dynamics. American Journal of Neuroradiology 31, 997–1002.
Hettiarachchi, H.D.M., Hsu, Y., Harris, T.J.j., Penn, R., Linninger, A.A., 2011. The effect of pulsatile flow on intrathecal drug delivery in the spinal canal. Annals of Biomedical Engineering 39, 2592–2602.
Hinokuma, K., Ohama, E., Oyanagi, K., Kakita, A., Kawai, K., Ikuta, F., 1992. Syringomyelia: a neuropathological study of 18 autopsy cases. Acta Pathologica Japonica 42, 25–34.
Hinsdale, G., 1897. Syringomyelia, an Essay to which was Awarded the Alvarenga Prize of the College of Philadelphia for the Year 1895. International Medical Magazine Co., Philadelphia.
Holmes, G., 1915. The Goulstonian Lectures on spinal injuries of warfare. I. The pathology of acute spinal injury. British Medical Journal 2, 769–774.
Hoskins, M.H., Kunz, R.F., Bistline, J.E., Dong, C., 2009. Coupled flow–structure–biochemistry simulations of dynamic systems of blood cells using an adaptive surface tracking method. Journal of Fluids and Structures 25, 936–953.
Howe, M.S., McGowan, R.S., 2009. Analysis of flow-structure coupling in a mechanical model of the vocal folds and the subglottal system. Journal of Fluids and Structures 25, 1299–1317.
Humphrey, J.D., 2003. Continuum biomechanics of soft biological tissues. Proceedings of the Royal Society of London: A 459, 3–46.
Hung, T.K., Chang, G.L., 1981. Biomechanical and neurological response of the spinal cord of a puppy to uniaxial tension. Journal of Biomechanical Engineering 103, 43–47.
Hung, T.K., Chang, G.L., Chang, J.L., Albin, M.S., 1981. Stress-strain relationship and neurological sequelae of uniaxial elongation of the spinal cord of cats. Surgical Neurology 15, 471–476.
Hung, T.K., Lin, H.S., Bunegin, L., Albin, M.S., 1982. Mechanical and neurological response of cat spinal cord under static loading. Surgical Neurology 17, 213–217.
Ichihara, K., Taguchi, T., Shimada, Y., Sakuramoto, I., Kawano, S., Kawai, S., 2001. Gray matter of the bovine cervical spinal cord is mechanically more rigid and fragile than the white matter. Journal of Neurotrauma 18, 361–367.
Joffroy, A., Achard, C., 1887. De la myélite cavitaire (observations; réflexions; pathogénie des cavités). Archives de Physiologie Normale et Pathologique 3, 435–472.
Johanson, C.E., 2008. Choroid plexus—cerebrospinal fluid circulatory dynamics: impact on brain, growth, metabolism, and repair, in: Conn, P.E. (Ed.), Neuroscience in Medicine, 3rd ed. Human Press, Totown, NJ, USA.
Josephson, A., Greitz, D., Klason, T., Olson, L., Spenger, C., 2001. A spinal thecal sac constriction model supports the theory that induced pressure gradients in the cord cause edema and cyst formation. Neurosurgery 48, 636–646.
Kalata, W., Martin, B.A., Oshinski, J.N., Jerosch-Herold, M., Royston, T.J., Loth, F., 2009. MR measurement of cerebrospinal fluid velocity wave speed in the spinal canal. IEEE Transactions on Biomedical Engineering 56, 1765–1768.
Kasantikul, V., Netsky, M.G., James, A.E., 1979. Relation of age and cerebral ventricle size to central canal in man. Journal of Neurosurgery 51, 85–93.
Klekamp, J., 2002. The pathophysiology of syringomyelia – historical overview and current

concept. Acta Neurochirurgica 144, 649–664.
Klekamp, J., 2009. Syringomyelia, in: Sindou, M. (Ed.), Practical Handbook of Neurosurgery. Springer Vienna, pp. 1260–1276.
Klekamp, J., Samii, M., 2002. Syringomyelia: Diagnosis and Treatment, 1st ed. Springer-Verlag, Berlin.
Koyanagi, I., Houkin, K., 2010. Pathogenesis of syringomyelia associated with Chiari type 1 malformation: review of evidences and proposal of a new hypothesis. Neurosurgical Review 33, 271–285.
Lederhaus, S.C., Pritz, M.B., Pribram, F.W., 1988. Septation in syringomyelia and its possible clinical significance. Neurosurgery 22, 1064–1067.
Levine, D.N., 2004. The pathogenesis of syringomyelia associated with lesions at the foramen magnum: a critical review of existing theories and proposal of a new hypothesis. Journal of the Neurological Sciences 220, 3–21.
Lichtenstein, B.W., 1943. Cervical syringomyelia and syringomyelia-like states associated with Arnold-Chiari deformity and platybasia. Archives of Neurology and Psychiatry 49, 881–894.
Linge, S.O., Haughton, V., Løvgren, A.E., Mardal, K.A., Langtangen, H.P., 2010. CSF flow dynamics at the craniovertebral junction studied with an idealized model of the subarachnoid space and computational flow analysis. American Journal of Neuroradiology 31, 185–192.
Lockey, P., Poots, G., Williams, B., 1975. Theoretical aspects of the attenuation of pressure pulses within cerebrospinal-fluid pathways. Medical and Biological Engineering 13, 861–869.
Lohle, P.N.M., Wurzer, H.A.L., Hoogland, P.H., Seelen, P.J., Go, K.G., 1994. The pathogenesis of syringomyelia in spinal cord ependymoma. Clinical Neurology and Neurosurgery 96, 323–326.
Loth, F., Yardimci, M.A., Alperin, N., 2001. Hydrodynamic modelling of cerebrospinal fluid motion within the spinal cavity. Journal of Biomechanical Engineering 123, 71–79.
Mack, J., Squier, W., Eastman, J.T., 2009. Anatomy and development of the meninges: implications for subdural collections and CSF circulation. Pediatric Radiology 39, 200–210.
Maikos, J.T., Elias, R.A.I., Shreiber, D.I., 2008. Mechanical properties of dura mater from the rat brain and spinal cord. Journal of Neurotrauma 25, 38–51.
Margaris, K.A., Black, R.A., 2012. Modelling the lymphatic system: challenges and opportunities. Journal of the Royal Society Interface 9, 601–612.
Marieb, E.N., 2000. Human Anatomy and Physiology. Benjamin Cummings.
Marmarou, A., Shulman, K., LaMorgese, J., 1975. Compartmental analysis of compliance and outflow resistance of the cerebrospinal fluid system. Journal of Neurosurgery 43, 523–534.
Martin, B.A., Labuda, R., Royston, T.J., Oshinski, J.N., Iskandar, B., Loth, F., 2010. Spinal subarachnoid space pressure measurements in an in vitro spinal stenosis model: implications on syringomyelia theories. Journal of Biomechanical Engineering 132, 111007-111001–111011.
Martin, B.A., Loth, F., 2009. The influence of coughing on cerebrospinal fluid pressure in an *in vitro* syringomyelia model with spinal subarachnoid space stenosis. Cerebrospinal Fluid Research 6, (18 pages).
Martin, B.A., Reymond, P., Novy, P., Baledent, O., Stergiopoulos, N., 2012. A coupled hydrodynamic model of the cardiovascular and cerebrospinal fluid system. American Journal of Physiology: Heart and Circulatory Physiology 302, H1492–H1509.
Martin, J.H., 2003. Neuroanatomy: Text and Atlas. McGraw Hill.
Martinez-Arizala, A., Mora, R.J., Madsen, P., Green, B.A., Hayashi, N., 1995. Dorsal spinal venous occlusion in the rat. Journal of Neurotrauma 12, 199–208.
Mazuchowski, E.L., Thibault, L.E., 2003. Biomechanical properties of the human spinal cord and pia mater, ASME Summer Bioengineering Conference. American Society of Mechanical Engineers, Florida, pp. 1205–1206.
McGrath, J.T., 1965. Spinal dysraphism in the dog with comments on syringomyelia.

Pathologia Veterinaria 2, 1–36.
Milhorat, T.H., Capocelli, A.L., Anzil, A.P., Kotzen, R.M., Milhorat, R.H., 1995. Pathological basis of spinal cord cavitation in syringomyelia: analysis of 105 autopsy cases. Journal of Neurosurgery 82, 802–812.
Milhorat, T.H., Capocelli, A.L., Kotzen, R.M., Bolognese, P., Heger, I.M., Cottrell, J.E., 1997. Intramedullary pressure in syringomyelia: clinical and pathophysiological correlates of syrinx distension. Neurosurgery 41, 1102–1110.
Milhorat, T.H., Chou, M.W., Trinidad, E.M., Kula, R.W., Mandell, M., Wolpert, C., Speer, M.C., 1999. Chiari I malformation redefined: clinical and radiographic findings for 364 symptomatic patients. Neurosurgery 44, 1005–1017.
Milhorat, T.H., Kotzen, R.M., Anzil, A.P., 1994. Stenosis of central canal of spinal cord in man: incidence and pathological findings in 232 autopsy cases. Journal of Neurosurgery 80, 716–722.
Morgagni, G.B., 1769. Of the hydrocephalus, and watry tumours of the spine, The Seats and Causes of Disease as Investigated by Anatomy (1761, tr. Alexander B). Miller & Candell Publishers, London, pp. Letter XII, Article 9, 255–257.
Moriwaki, F., Tashiro, K., Tachibana, S., Yada, K., 1995. [Epidemiology of syringomyelia in Japan—the nationwide survey]. Rinsho Shinkeigaku 35, 1395–1397.
Nash, M.P., Hunter, P.J., 2000. Computational mechanics of the heart. Journal of Elasticity 61, 113–141.
Netter, F.H., 1953. The nervous system, in: Netter, F.H. (Ed.), The Ciba Collection of Medical Illustrations. Ciba Pharmaceutical Products, New Jersey, p. 44.
Nicholas, D.S., Weller, R.O., 1988. The fine anatomy of the human spinal meninges. Journal of Neurosurgery 69, 276–282.
Nicholson, C., 1999. Structure of extracellular space and physiochemical properties of molecules governing drug movement in brain and spinal cord, in: Yaksh, T.L. (Ed.), Spinal Drug Delivery. Elsevier Science, Amsterdam, pp. 253–269.
Nolte, J., 2002. The Human Brain: An Introduction to its Functional Anatomy. Mosby, St. Louis.
Oakland, R.J., Hall, R.M., Wilcox, R.K., Barton, D.C., 2006. The biomechanical response of spinal cord tissue to uniaxial loading. Proceedings of the Institution of Mechanical Engineers, Part H: Journal of Engineering in Medicine 220, 489-492.
Odéen, H., Uppman, M., Markl, M., Spottiswoode, B.S., 2011. Assessing cerebrospinal fluid flow connectivity using 3D gradient echo phase contrast velocity encoded MRI. Physiological Measurement 32, 407–421.
Oldfield, E.H., Muraszko, K., Shawker, T.H., Patronas, N.J., 1994. Pathophysiology of syringomyelia associated with Chiari I malformation of the cerebellar tonsils. Implications for diagnosis and treatment. Journal of Neurosurgery 80, 3–15.
Ollivier D'Angers, C.P., 1827. Traité de la moelle épinière et de ses maladies: contenant l'histoire anatomique, physiologique et pathologique de ce centre nerveux chez l'homme. Chez Crevot, Paris.
Ouyang, H., Galle, B., Li, J., Nauman, E., Shi, R., 2008. Biomechanics of spinal cord injury: a multimodal investigation using ex vivo guinea pig spinal cord white matter. Journal of Neurotrauma 25, 19–29.
Ozawa, H., Matsumoto, T., Ohashi, T., Sato, M., Kokubun, S., 2001. Comparison of spinal cord gray matter and white matter softness: measurement by pipette aspiration method. Journal of Neurosurgery: Spine 95, 221–224.
Ozawa, H., Matsumoto, T., Ohashi, T., Sato, M., Kokubun, S., 2004. Mechanical properties and function of the spinal pia mater. Journal of Neurosurgery (Spine) 1, 122–127.
Païdoussis, M.P., 2004. Fluid-Structure Interactions – Slender Structures and Axial Flow, Volume 2. Elsevier Academic Press, London.
Park, E.-H., Dombrowski, S., Luciano, M., Zurakowski, D., Madsen, J.R., 2010. Alterations of

pulsation absorber characteristics in experimental hydrocephalus. Journal of Neurosurgery: Pediatrics 6, 159–170.
Parkinson, D., 1991. Human spinal arachnoid septa, trabeculae, and "rogue strands". American Journal of Anatomy 192, 498–509.
Patin, D.J., Eckstein, E.C., Harum, K., Pallares, V.S., 1993. Anatomic and biomechanical properties of human lumbar dura mater. Anesthesia and Analgesia 76, 535–540.
Persson, C., Summers, J., Hall, R.M., 2011. The importance of fluid-structure interaction in spinal trauma models. Journal of Neurotrauma 28, 113–125.
Peskin, C.S., 2002. The immersed boundary method. Acta Numerica 11, 479–517.
Pillay, P.K., Awad, I.A., Little, J.R., Hahn, J.F., 1991. Symptomatic Chiari malformation in adults: a new classification based on magnetic resonance imaging with clinical and prognostic significance. Neurosurgery 28, 639–645.
Redzic, Z.B., Preston, J.E., Duncan, J.A., Chodobski, A., Szmydynger-Chodobska, J., 2005. The choroid plexus-cerebrospinal fluid system: from development to aging, in: Schatten, G.P. (Ed.), Current Topics in Developmental Biology. Academic Press.
Reina, M.A., Casasola, O.D.L., Villanueva, M.C., Lopez, A., Maches, F., De Andres, J.A., 2004. Ultrastructural findings in human spinal pia mater in relation to subarachnoid anesthesia. Anesthesia and Analgesia 98, 1479–1485.
Rennels, M.L., Gregory, T.F., Blaumanis, O.R., Fujimoto, K., Grady, P.A., 1985. Evidence for a 'paravascular' fluid circulation in the mammalian central nervous system, provided by the rapid distribution of tracer protein throughout the brain from the subarachnoid space. Brain Research 326, 47–63.
Rice-Edwards, J.M., 1977. A pathological study of syringomyelia. Journal of Neurology, Neurosurgery and Psychiatry 40, 198.
Riley, H.A., 1930. Syringomyelia or myelodysplasia. The Journal of Nervous and Mental Disease 72, 1–27.
Roldan, A., Weiben, O., Haughton, V., Osswald, T., Chester, N., 2009. Characterization of CSF hydrodynamics in the presence and absence of tonsillar ectopia by means of computational flow analysis. American Journal of Neuroradiology 30, 941–946.
Roosen, N., Dahlhaus, P., Lumenta, C.B., Lins, E., Stork, W., Gahlen, D., Bock, W.J., 1988. Magnetic resonance (MR) imaging in the management of primary and secondary syringomyelic cavities, and of other cystic lesions of the spinal cord. Acta Neurochirurgica Supplement (Wien) 43, 13–16.
Runza, M., Pietrabissa, R., Mantero, S., Albani, A., Quaglini, V., Contro, R., 1999. Lumbar dura mater biomechanics: experimental characterization and scanning electron microscopy observations. Anesthesia and Analgesia 88, 1317–1321.
Saadoun, S., Papadopoulos, M.C., 2010. Aquaporin-4 in brain and spinal cord oedema. Neuroscience 168, 1036–1046.
Sakushima, K., Tsuboi, S., Yabe, I., Hida, K., Terae, S., Uehara, R., Nakano, I., Sasak, H., 2011. Nationwide survey on the epidemiology of syringomyelia in Japan. Journal of the Neurological Sciences 313, 147–152.
Samii, M., Klekamp, J., 1994. Surgical results of 100 intramedullary tumors in relation to accompanying syringomyelia. Neurosurgery 35, 865–873.
Sanan, A., van Loveren, H.R., 1999. The arachnoid and the myth of Arachne. Neurosurgery 45, 152–157.
Santini, F., Wetzel, S.G., Bock, J., Markl, M., Scheffler, K., 2009. Time-resolved three-dimensional (3D) phase-contrast (PC) balanced steady-state free precession (bSSFP). Magnetic Resonance in Medicine 62, 966–974.
Saxena, T., Gilbert, J.L., Hasenwinkel, J.M., 2009. A versatile mesoindentation system to evaluate the micromechanical properties of soft, hydrated substrates on a cellular scale. Journal of Biomedical Materials Research Part A 90, 1206–1217.

Shaffer, N., Martin, B.A., Loth, F., 2011. Cerebrospinal fluid hydrodynamics in type I Chari malformation. Neurological Research 33, 247–260.
Smillie, A., Sobey, I., Molnar, Z., 2005. A hydroelastic model of hydrocephalus. Journal of Fluid Mechanics 539, 417–442.
Sparrey, C.J., Keaveny, T.M., 2011. Compression behavior of porcine spinal cord white matter. Journal of Biomechanics 44, 1078–1082.
Speer, M.C., Enterline, D.S., Mehltretter, L., Hammock, P., Joseph, J., Dickerson, M., Ellenbogen, R.G., Milhorat, T.H., Hauser, M.A., George, T.M., 2003. Chiari type I malformation with or without syringomyelia: prevalence and genetics. Journal of Genetic Counseling 12, 297–311.
Stettler, J.C., Fazle Hussain, A.K.M., 1986. On transition of the pulsatile pipe flow. Journal of Fluid Mechanics 170, 169–197.
Stockman, H.W., 2006. Effect of anatomical fine structure on the flow of cerebrospinal fluid in the spinal subarachnoid space. Journal of Biomechanical Engineering 128, 106–114.
Stockman, H.W., 2007. Effect of anatomical fine structure on the dispersion of solutes in the spinal subarachnoid space. Journal of Biomechanical Engineering 129, 666–675.
Stoodley, M.A., Brown, S.A., Brown, C.J., Jones, N.R., 1997. Arterial pulsation-dependent perivascular cerebrospinal fluid flow into the central canal in the sheep spinal cord. Journal of Neurosurgery 86, 686–693.
Stoodley, M.A., Gutschmidt, B., Jones, N.R., 1999. Cerebrospinal fluid flow in an animal model of noncommunicating syringomyelia. Neurosurgery 44, 1065–1077.
Stoodley, M.A., Jones, N.R., Brown, C.J., 1996. Evidence for rapid fluid flow from the subarachnoid space into the spinal cord central canal in the rat. Brain Research 707, 155–164.
Stoodley, M.A., Jones, N.R., Yang, L., Brown, C.J., 2000. Mechanisms underlying the formation and enlargement of noncommunicating syringomyelia: experimental studies. Neurosurgical Focus 8, 1–7.
Storer, K.P., Toh, J., Stoodley, M.A., Jones, N.R., 1998. The central canal of the human spinal cord: a computerised 3-D study. Journal of Anatomy 192, 565–572.
Sweetman, B., Linninger, A.A., 2011. Cerebrospinal fluid flow dynamics in the central nervous system. Annals of Biomedical Engineering 39, 484–496.
Takizawa, H., Gabra-Sanders, T., Miller, J.D., 1986. Spectral analysis of the CSF pulse wave at different locations in the craniospinal axis. Journal of Neurology, Neurosurgery and Psychiatry 49, 1135–1141.
Tarlov, I.M., Klinger, H., Vitale, S., 1953. Spinal cord compression studies. Experimental techniques to produce acute and gradual compression. Archives of Neurology and Psychiatry 70, 813–819.
Tauber, E.S., Langworthy, O.R., 1935. A study of syringomyelia and the formation of cavities in the spinal cord. Journal of Nervous and Mental Disease 81, 245–264.
Tencer, A.F., Allen, B.L., Ferguson, R.L., 1985. A biomechanical study of thoracolumbar spinal fractures: part III. mechanical properties of the dura and its tethering ligaments. Spine 10, 741–747.
Tu, J., Liao, J., Stoodley, M.A., Cunningham, A.M., 2010. Differentiation of endogenous progenitors in an animal model of post-traumatic syringomyelia. Spine 35, 1116–1121.
Tu, J., Liao, J., Stoodley, M.A., Cunningham, A.M., 2011. Reaction of endogenous progenitor cells in a rat model of posttraumatic syringomyelia. Journal of Neurosurgery: Spine 14, 573–582.
Tubbs, R.S., Salter, G., Grabb, P.A., Oakes, W.J., 2001. The denticulate ligament: anatomy and functional significance. Journal of Neurosurgery 94, 271–275.
Tully, B., Ventikos, Y., 2011. Cerebral water transport using multiple-network poroelastic theory: application to normal pressure hydrocephalus. Journal of Fluid Mechanics 667, 188–215.
Tunturi, A.R., 1977. Elasticity of the spinal cord dura in the dog. Journal of Neurosurgery 47, 391–396.

Tunturi, A.R., 1978. Elasticity of the spinal cord, pia, and denticulate ligament in the dog. Journal of Neurosurgery 48, 975–979.
Urayama, K., 1994. Origin of lumbar cerebrospinal fluid pulse wave. Spine 19, 441–445.
Vandenabeele, F., Creemers, J., Lambrichts, I., 1996. Ultrastructure of the human spinal arachnoid mater and dura mater. Journal of Anatomy 189, 417–430.
Wagshul, M.E., Chen, J.J., Egnor, M.R., McCormack, E.J., Roche, P.E., 2006. Amplitude and phase of cerebrospinal fluid pulsations: experimental studies and review of the literature. Journal of Neurosurgery 104, 810–819.
Watton, P.N., Luo, X.-Y., Yin, M., Bernacca, G.M., Wheatley, D.J., 2008. Effect of ventricle motion on the dynamic behaviour of chorded mitral valves. Journal of Fluids and Structures 24, 58–74.
Wester, K., Kjosavik, I.-F., Midgard, R., 1989. Multicystic syringomyelia treated with a single, non-valved syringoperitoneal shunt: fast and near-complete MRI normalization. Acta Neurochirurgica Supplement (Wien) 98, 148–152.
Wiedemayer, H., Nau, H.E., Raukut, F., Gerhard, L., Reinhard, V., Grote, W., 1990. Pathogenesis and operative treatment of syringomyelia. Advances in Neurosurgery 18, 119–125.
Wilcox, R.K., Bilston, L.E., Barton, D.C., Hall, R.M., 2003. Mathematical model for the viscoelastic properties of dura mater. Journal of Orthopaedic Science 8, 432–434.
Williams, B., 1969. The distending force in production of communicating syringomyelia. The Lancet 2, 189–193.
Williams, B., 1970. Current concepts of syringomyelia. British Journal of Hospital Medicine 4, 331–342.
Williams, B., 1972. Combined cisternal and lumbar pressure recordings in the sitting position using differential manometry. Journal of Neurology, Neurosurgery and Psychiatry 35, 142–143.
Williams, B., 1974. A demonstration analogue for ventricular and intraspinal dynamics (DAVID). Journal of the Neurological Sciences 23, 445–461.
Williams, B., 1976. Cerebrospinal fluid pressure changes in response to coughing. Brain 99, 331–346.
Williams, B., 1980. On the pathogenesis of syringomyelia: a review. Journal of the Royal Society of Medicine 73, 798–806.
Williams, B., 1986. Progress in syringomyelia. Neurological Research 8, 130–145.
Williams, B., 1990. Syringomyelia. Neurosurgery Clinics of North America 1, 653–685.
Wong, J., Hemley, S., Jones, N., Cheng, S., Bilston, L., Stoodley, M., 2012. Fluid outflow in a large-animal model of posttraumatic syringomyelia. Neurosurgery 71, 474–480.
Yamada, S., Won, D.J., Pezeshkpour, G., Yamada, B.S., Yamada, S.M., Siddiqi, J., Zouros, A., Colohan, A.R.T., 2007. Pathophysiology of tethered cord syndrome and similar complex disorders. Neurosurgical Focus 23, E6-1–10.
Yang, L., Jones, N.R., Stoodley, M.A., Blumbergs, P.C., Brown, C.J., 2001. Excitotoxic model of post-traumatic syringomyelia in the rat. Spine 26, 1842–1849.
Yang, S., Yang, X., Hong, G., 2009. Surgical treatment of one hundred seventy-four intramedullary spinal cord tumors. Spine 34, 2705–2710.
Zarzur, E., 1996. Mechanical properties of the human lumbar dura mater. Arquivos de Neuro-Psiquiatria 54, 455–460.
Zhang, E.T., Inman, C.B.E., Weller, R.O., 1990. Interrelationships of the pia mater and the perivascular (Virchow-Robin) spaces in the human cerebrum. Journal of Anatomy 170, 111–123.

(a)

(b)

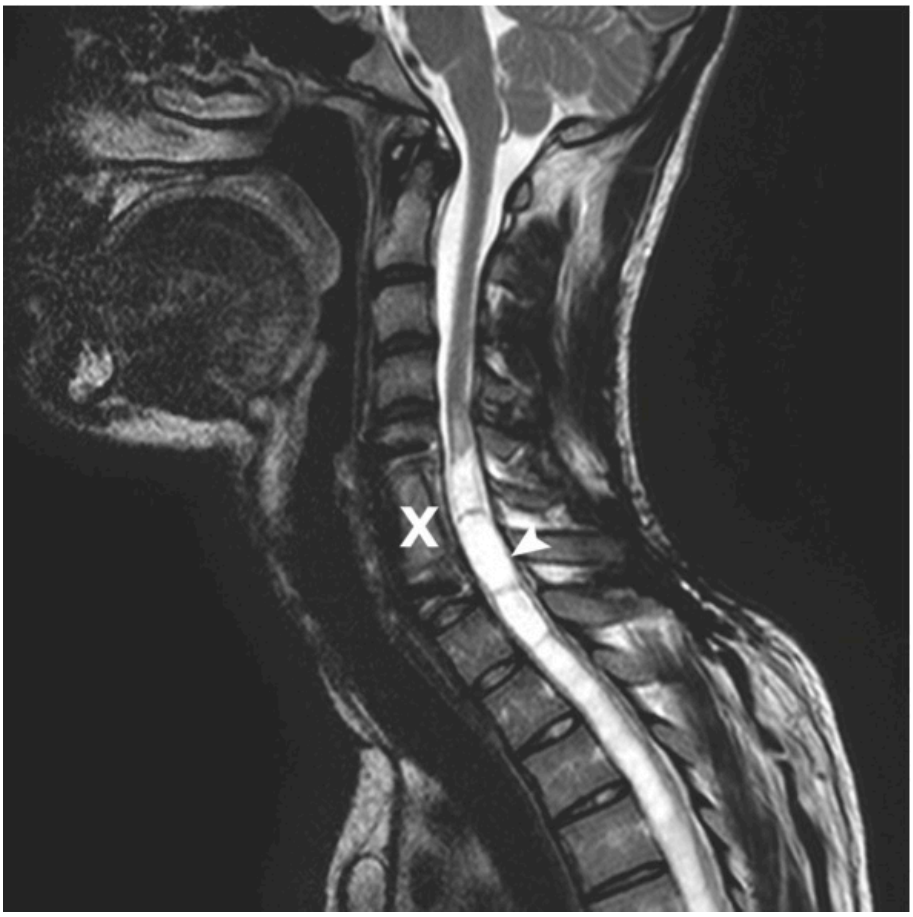

(c)

Fig. 1. T2-weighted saggital MR images showing syrinxes in association with (a,b) Chiari malformation, and (c) spinal injury. (a) In this 37-year-old patient who presented with headache the cerebellar tonsil (*) lies low in the foramen magnum but CSF (white on this image) is seen around the tonsil. A prominent central canal (arrow head), or early syrinx, is seen. At this time analgesia alone controlled the symptoms. (b) Four years later the patient developed hand weakness and arm pain. The repeat MRI shows the cerebellar tonsil (*) with no CSF surrounding and a new syrinx (arrow head) and cord oedema rostral and caudal to the syrinx. (c) MRI of a patient following a significant spinal cord injury. The site of a bone graft used to stabilize and repair the vertebral column is shown (X). The patient developed worsening pain and motor function. The syrinx that has developed is shown (arrowhead).

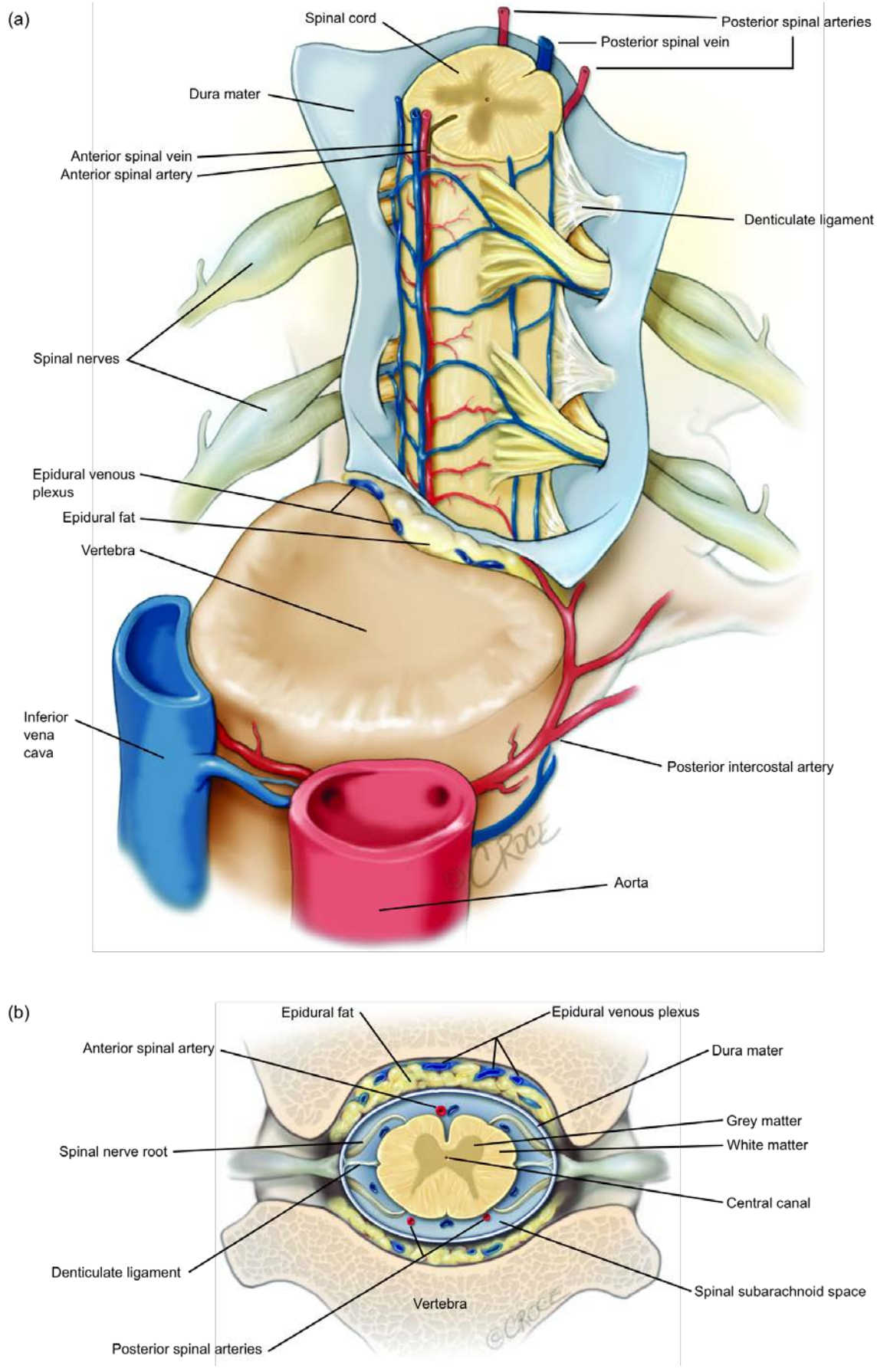

Fig. 2. Gross anatomy of the spinal cord featuring the meninges. (a) depicts the cord in its location within the vertebrae and (b) is a cross-sectional view in which the cord is cut at a level slightly higher than the vertebra.

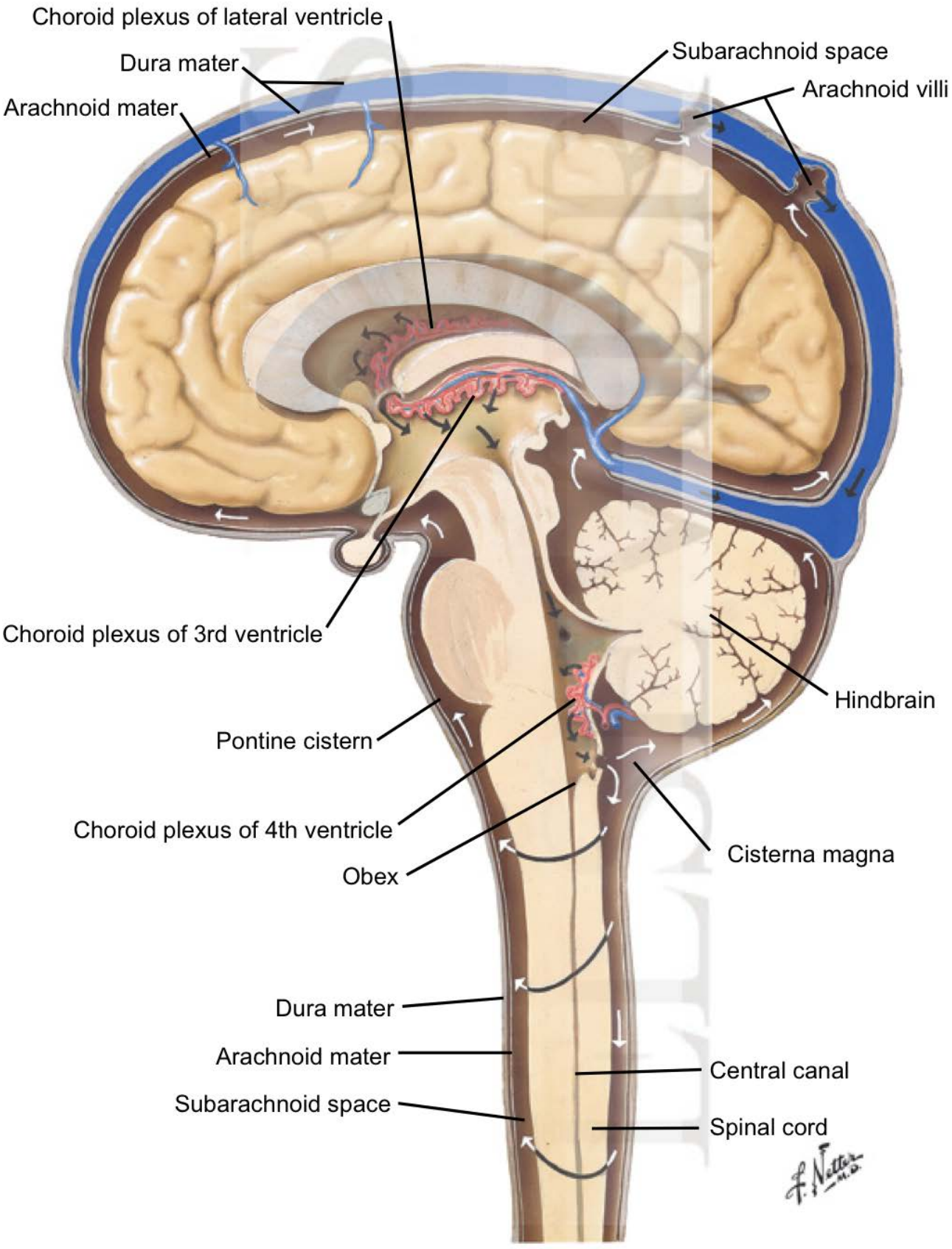

Fig. 3. Pathways of CSF flow. Reproduced with permission from Netter (1953).

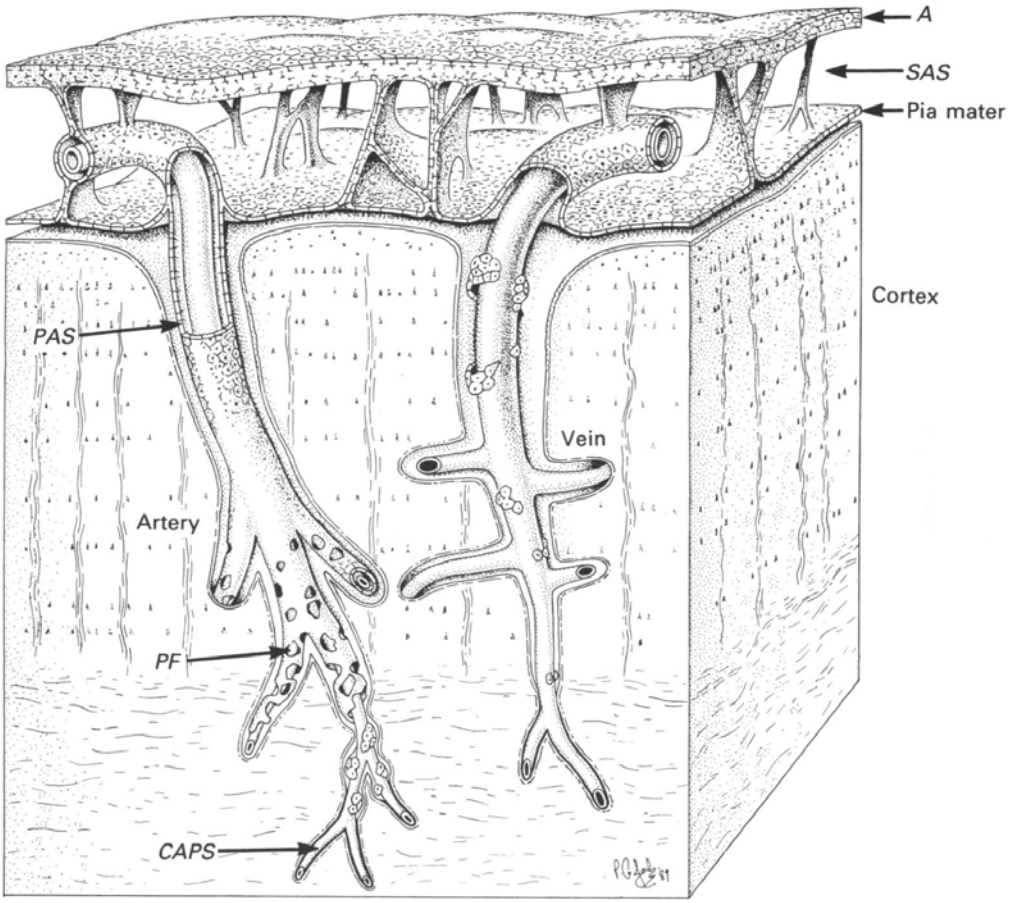

Fig. 4. Schematic diagram showing the fluid spaces on either side of the cranial pial membrane. The situation of the spinal pial membrane and surrounding fluids is thought to be similar although this is not known for certain. Slightly different notation to the text is used here: A = arachnoid mater, SAS = subarachnoid space, PAS = periarterial space, PF = perforated, CAPS = capillary. Note the pia-like sheaths around both blood vessels, which is lost in the cortex in the case of the vein, their perforations and the subpial fluid space along the cortex surface. Not shown are the leaky gap junctions in the pial membrane that also permit fluid to be exchanged between the SAS and the PVS. Reproduced with permission from Zhang et al. (1990), figure 10.

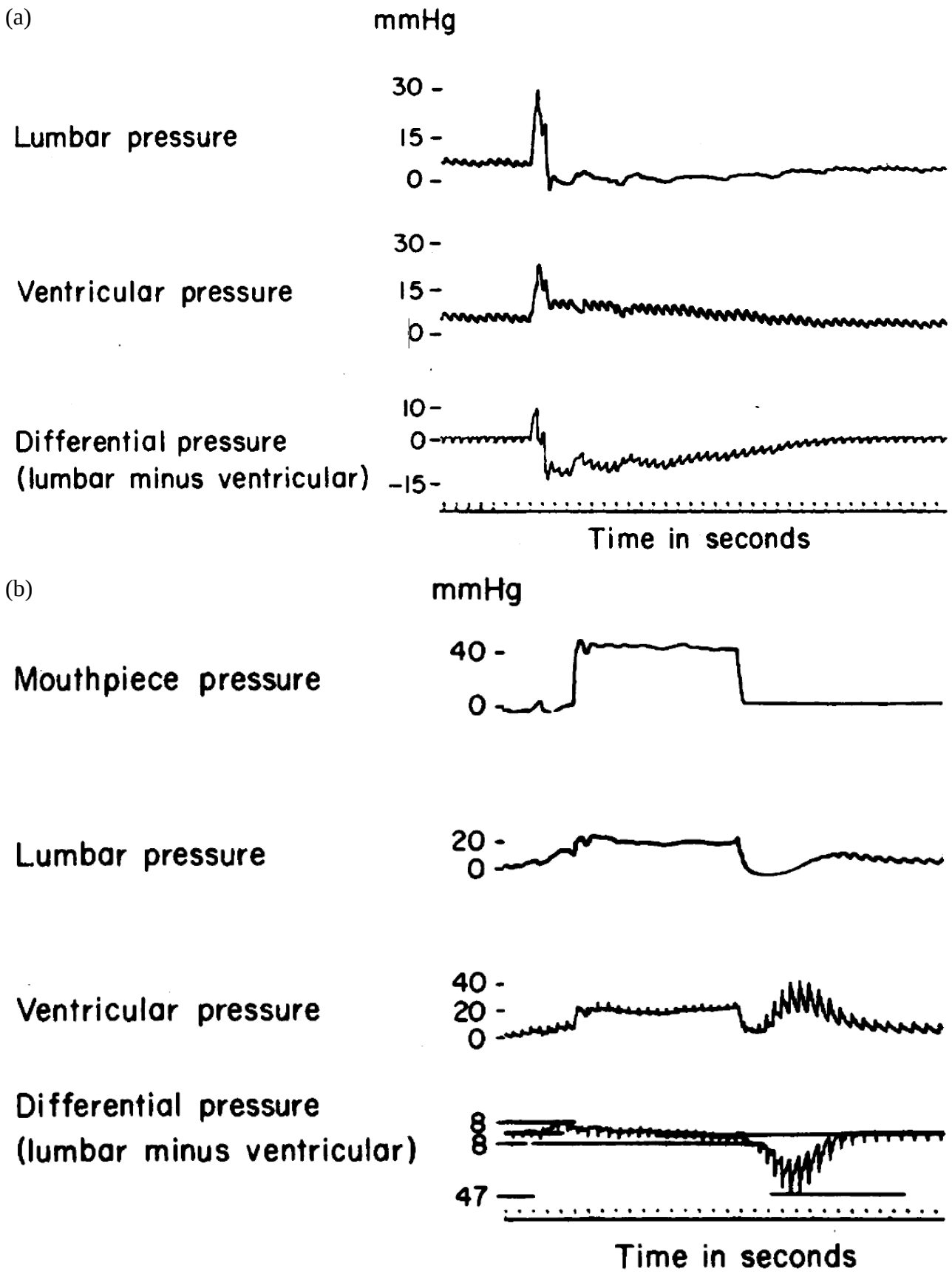

Fig. 5. Pressure dissociation following (a) a cough and (b) a Valsalva manoeuvre. See text for detailed explanation. Panels (a) and (b) reproduced with permission from Williams (1980), figures 1 and 2 respectively.

References

Netter, F.H., 1953. The nervous system, in: Netter, F.H. (Ed.), The Ciba Collection of Medical Illustrations. Ciba Pharmaceutical Products, New Jersey, p. 44.

Williams, B., 1980. On the pathogenesis of syringomyelia: a review. Journal of the Royal Society of Medicine 73, 798–806.

Zhang, E.T., Inman, C.B.E., Weller, R.O., 1990. Interrelationships of the pia mater and the perivascular (Virchow-Robin) spaces in the human cerebrum. Journal of Anatomy 170, 111–123.